FUSION OF HIGH-RESOLUTION SATELLITE IMAGES

by

YANGRONG LING

(Under the Direction of E. Lynn Usery)

ABSTRACT

Two advanced image fusion techniques, a fast Fourier transform (FFT)-enhanced intensity-hue-saturation (IHS) transform method and a wavelet-enhanced IHS transform method, are developed for fusing commercial high-resolution satellite images. Instead of using a total replacement of the intensity component as in the traditional IHS transform method, the FFT-enhanced IHS transform method uses a partial replacement based on FFT filtering. The wavelet-enhanced IHS transform method combines the traditional IHS transform and a discrete wavelet transform. It uses a partial replacement based on a wavelet-based technique, where only the high frequency part of the panchromatic image is fused to the multispectral image. Ikonos and QuickBird image data are used to assess these two enhanced IHS methods. Visual and statistical comparisons of the fused images demonstrate that the enhanced IHS methods produce better results than the traditional IHS transform and principal components analysis (PCA) methods in preserving the spectral characteristics of the input multispectral image while inheriting the spatial details of the panchromatic data.

This research also assesses how the resolution ratio, defined as the ratio between the spatial resolution of the high-resolution panchromatic image and that of the low-resolution multispectral image, affects the quality of the fused image. It has been shown that a resolution

ratio of 1:10 or better (e.g., 1:5) is needed for successful multisensor image fusion provided the panchromatic image is not resampled to a coarser resolution. Generally, the quality of the fused image decreases as the resolution ratio decreases (e.g., from 1:10 to 1:30). However, even with a resolution ratio as small as 1:30, the fused image is still better than the original multispectral image alone. On the other hand, due to the synthetic pixels generated in resampling, more artifacts are introduced in the fused image as the resolution ratio decreases. In some cases, when the resolution ratio is small, e.g., 1:30, one might need to adjust the spatial resolution of the fused image to obtain better spectral quality by resampling the high spatial resolution panchromatic image to a slightly lower resolution before fusing it with the multispectral image.

INDEX WORDS: Image Fusion, FFT, Wavelet Transform, IHS Transform, PCA, Resolution Ratio, Ikonos, QuickBird

FUSION OF HIGH-RESOLUTION SATELLITE IMAGES

by

YANGRONG LING

B.S., Changchun University of Earth Science, China, 1994

M.S., Chinese Academy of Sciences, China, 1997

M.S., University of Georgia, 2003

A Dissertation Submitted to the Graduate Faculty of The University of Georgia in Partial Fulfillment of the Requirements for the Degree

DOCTOR OF PHILOSOPHY

ATHENS, GEORGIA

2006

FUSION OF HIGH-RESOLUTION SATELLITE IMAGES

by

YANGRONG LING

Major Professor: E. Lynn Usery

Committee: Hamid Arabnia
Marguerite Madden
Clifton W. Pannell
Roy A. Welch

Electronic Version Approved:

Maureen Grasso
Dean of the Graduate School
The University of Georgia
May 2006

DEDICATION

To my Mom and Dad

ACKNOWLEDGEMENTS

I am deeply indebted to Dr. E. Lynn Usery, my major professor, whose generous help, encouragement, and expert guidance were responsible for the completion of this dissertation. Special recognition is also given to Dr. Roy A. Welch for his invaluable contributions and guidance in the early stages of the research and preparation of this dissertation. My sincere thanks as well go to the rest of my graduate committee, Dr. Marguerite Madden, Dr. Hamid Arabnia, and Dr. Clifton Pannell for their timely assistance and valuable suggestions. A very special thanks goes to Dr. Manfred Ehlers for his valuable suggestions and collaboration of some of the research work.

Support for the Ikonos, QuickBird, and other image data was provided by the Center for Remote Sensing and Mapping Science (CRMS), The University of Georgia and the National Geospatial-Intelligence Agency (NGA) (formerly National Imagery and Mapping Agency) (NIMA)) under the Cooperative Agreement NMA 201-00-1-1006, Assessing the Ability of Commercial Sensors to Satisfy Littoral Warfare Data Requirements. I would like to express my appreciation to Dr. Richard Brand and Dr. Scott Loomer for their initiative and assistance throughout the project. I also gratefully acknowledge Dr. Thomas Jordan for his help in image processing and other research work. My appreciation is also expressed to Virginia Vickery for her friendship and excellent management work. Sincere appreciation is also extended to all other scientists, co-workers, and fellow graduate students at the CRMS, for their kindness, help, and support.

I also like to thank my parents in law, Xingjia Lu and Yulan Chou, for taking good care of my son during the past two years. Finally, I wish to express my deepest gratitude to my wife, QiQi Lu, and my son, Evan, for their constant support and patience. I am profoundly grateful for their love, encouragement, and endurance.

TABLE OF CONTENTS

LIST OF TABLES

Page

LIST OF FIGURES

Page

CHAPTER 1

INTRODUCTION

Background

The launch of the new generation of commercial satellites for high resolution remote sensing marks the start of a new era of space imaging for earth observation (Fritz 1996). Among several commercial high-resolution imaging satellites, Ikonos of Space Imaging Inc., QuickBird of DigitalGlobe Inc., and OrbView-3 of Orbimage Inc., were successfully launched in 1999, 2001, and 2003, respectively (Table 1.1). These satellites provide spatial resolution in the one-meter range compared to medium and low resolution of the previous satellite imaging systems (Table 1.2). The high-resolution images from these commercial satellites currently can be acquired in two different modes: a panchromatic (Pan) mode with a high spatial resolution and a multispectral (XS) mode with a slightly coarser resolution. To effectively utilize such images, techniques that can effectively combine the high-resolution panchromatic and low-resolution multispectral images into one color image are needed. Such techniques can largely extend the application potential of remote sensing image data.

The fusion of high-resolution panchromatic and low-resolution multispectral satellite images is a very important issue for many remote sensing and mapping applications (Zhang 2002). It is the aim of image fusion to integrate image data recorded at different resolutions or by different sensors in order to obtain more information than can be derived from a single image alone (Pohl and Van Genderen 1998). There are many situations in remote sensing that simultaneously require high spatial and high spectral resolution in a single image. By combining

Table 1.1: Currently Operational Commercial High-Resolution Satellites (Source: ERSC 2005; Updated as of February 18, 2005).

Satellite name	Source	Launch	Sensors	Types	Spectral Bandwidth (μm)	Resolution (meters)
Ikonos	Space Imaging	9/24/1999	Ikonos	Pan	0.45 – 0.90	1
				XS	0.45 – 0.52	4
					0.51 – 0.60	
					0.63 – 0.70	
					0.76 – 0.85	
QuickBird	DigitalGlobe	10/18/2001	QuickBird	Pan	0.45 – 0.90	0.61
				XS	0.45 – 0.52	2.44
					0.52 – 0.60	
					0.63 – 0.69	
					0.76 – 0.85	
Orbview-3	Orbimage	6/26/2003	Orbview	Pan	0.45 – 0.90	1
				XS	0.45 – 0.52	4
					0.52 – 0.60	
					0.625 – 0.685	
					0.76 – 0.90	

Table 1.2: Classification of the Spatial Resolutions of Satellite Imagery (Fritz 1999).

Very Low	≥ 300 m
Low	≥ 30 to < 300 m
Medium	≥ 3 to < 30 m
High	≥ 0.5 to < 3 m
Very High	< 0.5 m

or fusing images it may be possible to obtain both high spatial and spectral resolution in a single display. The benefit of image fusion has been demonstrated in many practical applications such as studies of urban analysis, vegetation, land-use, and precision farming (Couloigner *et al.* 1998, Dai and Khorram 1999, Kurz 2000, Lau 2000, Tu *et al.* 2001, Chen *et al.* 2003, Sun *et al.* 2003).

A variety of image fusion techniques have been developed, applied, and assessed over the past two decades (e.g., Cliche *et al.* 1985, Price 1987, Welch and Ehlers 1987, Chavez *et al.* 1991, Ehlers 1991, Shettigara 1992, Yesou *et al.* 1994, Zhou *et al.* 1998, Zhang 2002). Most techniques are reported for successful fusion of radar or *Système Pour l'Observation de la Terre* (SPOT) panchromatic images with other multispectral images, such as Landsat Thematic Mapper (TM) and SPOT High Resolution Visible (HRV) multispectral images. Among the existing fusion techniques, the intensity-hue-saturation (IHS) transform and principal components analysis (PCA) methods are most effective and have been widely used in the remote sensing community (Zhang 1999, Tu *et al.* 2001). However, existing techniques may not satisfy conditions for successful fusion of the new generation satellite images such as Ikonos and QuickBird due to the wavelength extension of the panchromatic images. A more significant color distortion often occurs in the fused image than traditional fusion of lower resolution images such as SPOT panchromatic and Landsat TM multispectral images (Zhang 2002). In addition, most previous work involved evaluation of the fused image only based on visual inspection. There are few quantitative comparisons of the spatial and spectral information content (Tu *et al.* 2001).

The resolution ratio in image fusion also affords evaluation. A resolution ratio of 1:30, for example, can be defined as the ratio between the pixel size of the high-resolution panchromatic image (e.g., Ikonos 1-m Pan) and that of the low-resolution multispectral image (e.g., Landsat TM 30-m XS). A resolution ratio of 1:10 is greater than a resolution ratio of 1:30. While previous work on image fusion mainly focused on the enhancement of spatial information and preservation of spectral characteristics, a fixed resolution ratio often is used in the fusion. The study of how resolution ratio affects the quality of the fused image, however, has been seldom reported.

Objectives

With commercial high-resolution satellite image data increasingly available to the geospatial community, the selection of methods for fusing panchromatic and multispectral images (also known as pan-sharpening) has become a critical issue. Although currently the vendors of the commercial high-resolution satellite image data such as Space Imaging and DigitalGlobe do provide pan-sharpened products to the customers, the algorithms are not open sources for the public and may warrant improvement. Consequently, the three major objectives of this study are:

(1) to develop two enhanced IHS transform methods: a fast Fourier transform (FFT)-enhanced IHS transform method and a wavelet-enhanced IHS transform method, for fusing commercial high-resolution satellite images acquired by Ikonos and QuickBird;

(2) to comprehensively assess the improvement in spatial resolution and the retention of spectral fidelity in the fused image; and

(3) to assess how the resolution ratio of input images affects the quality of the fused image.

In order to meet the above objectives, this dissertation is structured to include a brief introduction to the study area and image data, a literature review, two manuscripts, and a summary and set of conclusions. The manuscripts focus on two enhanced IHS transform methods for fusing high-resolution satellite images and how the resolution ratio affects the quality of the fused image. They will be submitted for publication in the *ISPRS Journal of Photogrammetry and Remote Sensing* and the *International Journal of Remote Sensing*, respectively.

Study Area and Image Data

The study area is located in Camp Lejeune, North Carolina (34° 35' N latitude, 77° 18' W longitude), the largest U.S. Marine Corps (USMC) Base in the world, occupying an area of 619 km^2 (Fleming 2004). It is located within Onslow County in the White Oak River Basin of the lower coastal plain of southeastern North Carolina (Figure 1.1). The Base is composed of 153,000 acres, containing 26,000 acres of surface water and 127,000 acres of land varying in elevation from sea level to 70 feet above sea level. Approximately 14,000 acres of land have been developed for administration, maintenance, logistics, and personnel support facilities. There are over 6,800 buildings and 450 miles of roads at Camp Lejeune, with the remaining land used primarily for military training (Brewer 2000).

Ikonos and QuickBird image data acquired over the Camp Lejeune study area are used for evaluating the fusion methods in Chapter 3. The Ikonos image data cover a complex region with sea, land, and air features, while the QuickBird image data cover a built-up area with urban features such as roads, buildings, and golf courses. Both datasets include a panchromatic band and three multispectral bands. In Chapter 4, an Ikonos dataset, a SPOT panchromatic image, and a Landsat Enhanced Thematic Mapper Plus (ETM+) multispectral image are used to examine the

effects of resolution ratio changes on image quality. Table 1.3 lists the details of the image data used in the study. All images are spatially registered to the Universal Transverse Mercator (UTM) coordinate system on the WGS 84 datum.

Table 1.3: Image Data Used in the Study

Image data	Spectral bandwidth (μm)	Spatial resolution (m)	Acquisition date
SPOT Pan	0.51 – 0.73	10	5/20/1996
Landsat-ETM+ XS (Bands 2, 3, 4)	Band 2: 0.53 – 0.61 Band 3: 0.63 – 0.69 Band 4: 0.78 – 0.90	30	9/23/1999
Ikonos Pan	0.45 – 0.90	1	2/5/2000
Ikonos XS (Bands 2, 3, 4)	Band 2: 0.51 – 0.60 Band 3: 0.63 – 0.70 Band 4: 0.76 – 0.85	4	8/27/2001
QuickBird Pan	0.45 – 0.90	0.61	3/3/2003
QuickBird XS (Bands 2, 3, 4)	Band 2: 0.52 – 0.60 Band 3: 0.63 – 0.69 Band 4: 0.76 – 0.85	2.44	3/24/2003

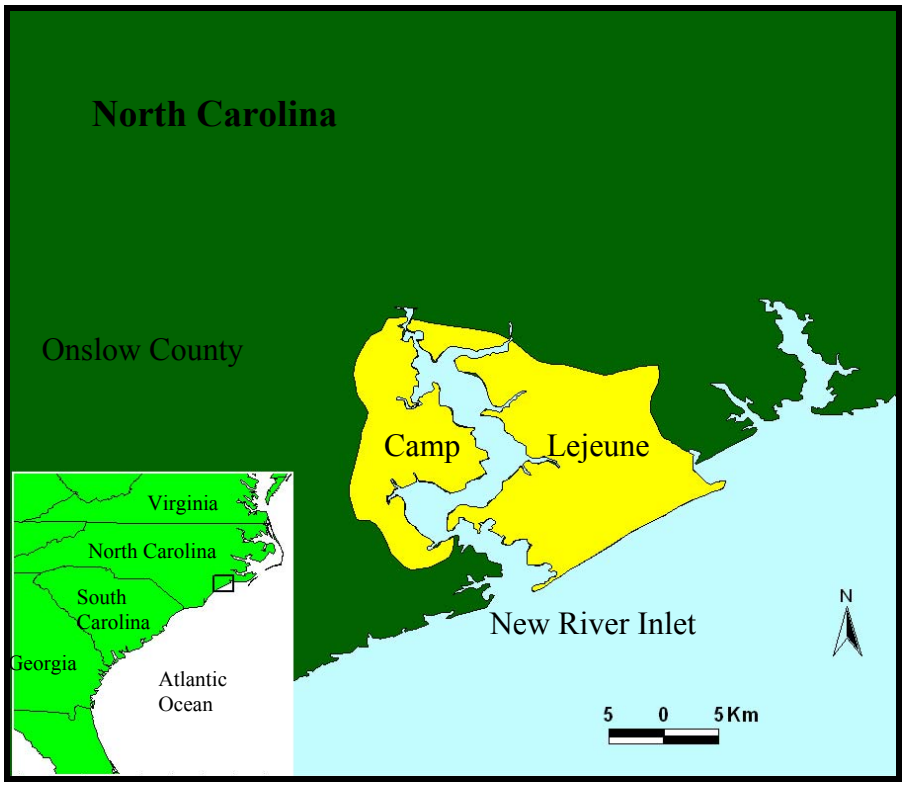

Figure 1.1: Camp Lejeune study area, North Carolina.

References

Brewer, S.A., 2000. Natural resources FY 2000: larger installation – Marine Corps Base Camp Lejeune, URL: https://www.denix.osd.mil/denix/Public/News/OSD/SecDef00/NR/mcbcamplejeunenrlargeinstallation.pdf (last date accessed: 23 November 2005).

Chavez, P.S., S.C. Sides, and J.A. Anderson, 1991. Comparison of three different methods to merge multiresolution and multispectral data: TM & SPOT pan, *Photogrammetric Engineering and Remote Sensing*, Vol. 57, No. 3, pp. 295 – 303.

Chen, C.M., G.F. Hepner, and R.R. Forster, 2003. Fusion of hyperspectral and radar data using the IHS transformation to enhance urban surface features, *ISPRS Journal of Photogrammetry and Remote Sensing*, Vol. 58, No. 1, pp. 19 – 30.

Cliche, G., F. Bonn, and P. Teillet, 1985. Integration of the SPOT Pan channel into its multispectral mode for image sharpness enhancement, *Photogrammetric Engineering and Remote Sensing*, Vol. 51, No. 3, pp. 311 – 316.

Couloigner, I., T. Ranchin, V. Valtonen, and L. Wald, 1998. Benefit of the future SPOT-5 and of data fusion to urban roads mapping, *International Journal of Remote Sensing*, Vol. 19, No. 8, pp. 1519 – 1532.

Dai, X. and S. Khorram, 1999. Data fusion using artificial neural networks: a case study on multitemporal change analysis, *Computers, Environment and Urban Systems*, Vol. 23, No. 1, pp. 19 – 31.

Ehlers, M., 1991. Multisensor image fusion techniques in remote sensing, *ISPRS Journal of Photogrammetry and Remote Sensing*, Vol. 46, No. 1, pp. 19 – 30.

ERCS, updated as of February 18, 2005. Earth observation satellites: current. *Environmental Remote Sensing Center*, *University of Wisconsin-Madison*, URL: http://www.ersc.wisc.edu/resources/EOSC.php (last date accessed: 20 November 2005).

Fleming, S., 2004. *Geospatial Information for Joint Military Operations in the Littoral Zone*, Ph.D. Dissertation, Department of Geography, The University of Georgia, May 2004, 110 p.

Fritz, L.W., 1996. The era of commercial earth observation satellites, *Photogrammetric Engineering and Remote Sensing*, Vol. 62, No. 1, pp. 39 – 45.

Fritz, L.W., 1999. Commercial Earth observation satellites. *Geomatics Information Magazine*, Vol. 13, No. 5, pp. 6 – 9.

Kurz, F., 2000. Empirical estimation of vegetation parameters using multisensor data fusion, *International Archives of Photogrammetry and Remote Sensing*, Vol. 33, Part 77/2, pp. 733 – 737.

Lau, W., 2000. The influences of image classification by fusion of spatially oriented images, *International Archives of Photogrammetry and Remote Sensing*, Vol. 33, Part 77/2, pp. 752 – 759.

Pohl, C. and J.L.Van Genderen, 1998. Multisensor image fusion in remote sensing: concepts, methods and applications, *International Journal of Remote Sensing*, Vol. 19, No. 5, pp. 823 – 854.

Price, J.C., 1987. Combining panchromatic and multispectral imagery from dual resolution satellite instruments, *Remote Sensing of Environment*, Vol. 21, No. 1, pp. 119 – 128.

Shettigara, V. K., 1992. A generalized component substitution technique for spatial enhancement of multispectral images using a higher resolution data set, *Photogrammetric Engineering and Remote Sensing*, Vol. 58, No. 5, pp. 561 – 567.

Sun, W., V. Heidt, P. Gong, and G. Xu, 2003. Signal and image processing – information fusion for rural land-use classification with high-resolution satellite imagery, *IEEE Transactions on Geoscience and Remote Sensing*, Vol. 41, No. 4, pp. 883 – 890.

Tu, T.M., S.C. Su, H.C. Shyu, and P.S. Huang, 2001. A new look at IHS-like image fusion methods, *Information Fusion*, Vol. 2, No. 3, pp. 177 – 186.

Welch, R. and M. Ehlers, 1987. Merging multiresolution SPOT HRV and Landsat TM data, *Photogrammetric Engineering and Remote Sensing*, Vol. 53, No. 3, pp. 301 – 303.

Yesou, H., Y. Besnus, and J. Rolet, 1994. Perception of a geological body using multiple source remotely-sensed data – relative influence of the spectral content and the spatial resolution, *International Journal of Remote Sensing*, Vol. 15, No. 12, pp. 2495 – 2510.

Zhang, Y., 1999. A new merging method and its spectral and spatial effects, *International Journal of Remote Sensing*, Vol. 20, No. 10, pp. 2003 – 2014.

Zhang, Y., 2002. Automatic image fusion: A new sharpening technique for Ikonos multispectral images, *GIM International*, Vol. 16, No. 5, pp. 54 – 57.

Zhou, J., D.L. Civco, and J.A. Silander, 1998. A wavelet transform method to merge Landsat TM and SPOT panchromatic data, *International Journal of Remote Sensing*, Vol. 19, No. 4, pp. 743 – 757.

CHAPTER 2

LITERATURE REVIEW OF IMAGE FUSION

Concept of Image Fusion

Image fusion is a tool to combine multi-source imagery using advanced image processing techniques. It aims at the integration of disparate and complementary data to enhance the information apparent in the images as well as to increase the reliability of the interpretation. This leads to more accurate data and increased utility. It is also stated that fused data provide for robust operational performance, i.e., increased confidence, reduced ambiguity, improved reliability and improved classification (Rogers and Wood 1990). A general definition of *image fusion* can be given as *'Image fusion is the combination of two or more different images to form a new image by using a certain algorithm'* (Van Genderen and Pohl 1994).

Depending on the stage at which fusion takes place, image fusion is often divided into three categories, namely, pixel level, feature level and decision level (Pohl and Van Genderen 1998). In pixel level fusion, the combination mechanism works directly on the pixels obtained at the sensors' outputs. Feature level fusion, on the other hand, works on image features extracted from the source images. Decision level fusion works at an even higher level, and merges the interpretations of different images obtained after image understanding (Figure 2.1). This study focuses on pixel level image fusion.

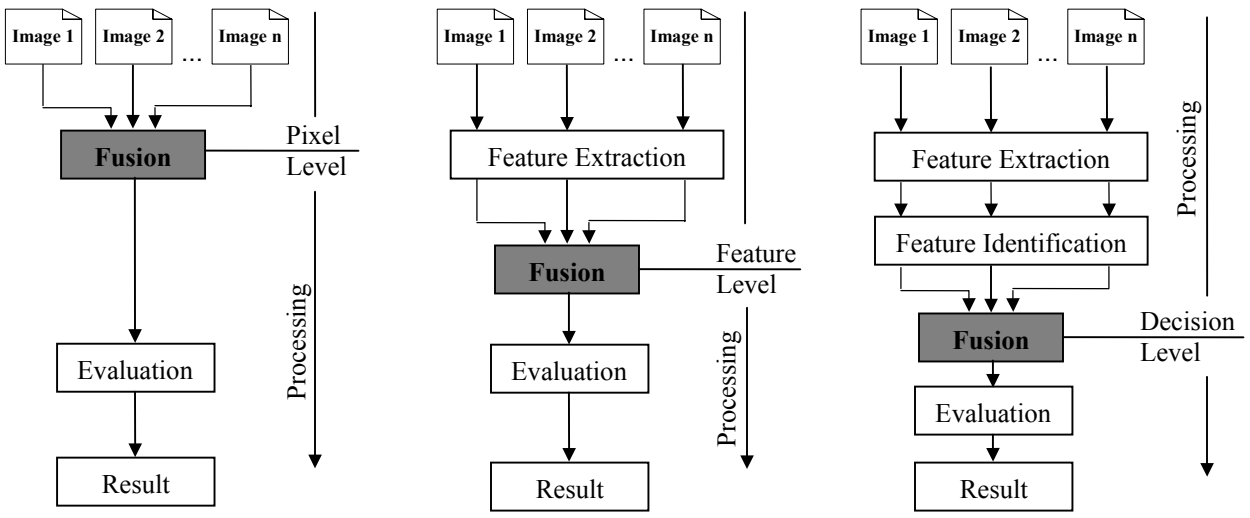

Figure 2.1: Processing levels of image fusion (Pohl and Van Genderen 1998).

Some other terms with similar meaning of image fusion can be found in the literature, such as *image merging*, *image combination*, *image synergy*, and *image integration*. Data fusion is another term closely related to image fusion and frequently used in the literature. It means a wider domain than image fusion and a variety of definitions have been proposed (Li *et al*. 1995, Hall and Llinas 1997). A search for a more suitable definition of data fusion was launched by the European Association of Remote Sensing Laboratories (EARSeL) and the French Society for Electricity and Electronics (SEE, French affiliate of the IEEE). The following definition was adopted in January 1998: "data fusion is a formal framework in which are expressed means and tools for the alliance of data originating from different sources. It aims at obtaining information of greater quality; the exact definition of 'greater quality' will depend upon the application" (Wald 1999).

Applications of Image Fusion

Image fusion techniques have been widely used in many applications in different fields, especially those that rely on information from different sensors. In the geosciences, there are an increasing number of applications in which multisensor images are used to improve and enhance image interpretation. This includes urban analysis, topographic mapping and map updating, land use/cover, hazards monitoring, and geology (Pohl and Van Genderen 1998).

Urban Analysis

It has been suggested that the most important technical issue in urban remote sensing is the spatial resolution of the image data (Welch 1982). With the development of new generation high-resolution satellite systems, many analysts are already working with data of a spatial resolution finer than 5 meters, and anticipating still greater discrimination of the urban fabric (Donnay *et al*. 2001). However, the majority of high-resolution images are presently recorded in panchromatic mode only. On the other hand, the different types of land use in an urban area can be better mapped if high spectral resolution data are available. The solutions suggested for solving this problem involve merging the higher resolution panchromatic data with lower resolution multispectral data (Jones *et al*. 1991, Ackerman 1995, Ranchin *et al.* 1996, Ranchin and Wald 2000).

Many successful works of urban analysis using image fusion have been published. For example, Couloigner *et al.* (1998) fused simulated SPOT-5 panchromatic and multispectral images for urban roads mapping. The result shows that the improvement of the spatial resolution from image fusion allows the detection of more urban roads. It has also been found that more information is extracted by photo-interpretation from the color composite of the fused multispectral image than from a panchromatic image of similar spatial resolution. Zhang and

Wang (2004) used a multi-resolution and multi-spectral image fusion for urban object extraction. Both spectral information from QuickBird multispectral images and spatial information from QuickBird panchromatic images were utilized for the extraction to improve accuracies. The results demonstrated that the completeness and correctness of roadwork extraction were significantly higher than those of other existing road extraction methods.

Topographic Mapping and Map Updating

Image fusion as a tool can provide up-to-date information for topographic mapping and map updating. Information about an observed object not covered by one sensor might be contained in the data from another. For example, the combination of the visible and infrared image with synthetic aperture radar (SAR) data are often used in the field of topographic mapping or map updating. The visible and infrared data serve as reference while the SAR data that can be acquired at any time provide the most recent situation. Welch and Ehlers (1988) fused a Shuttle Imaging Radar-B (SIR-B) image with a Landsat TM multispectral image for cartographic feature extraction. It shows that the completeness of cartographic features extracted from the fused image exceeded those obtained from separate SIR-B and TM image data sets by approximately 10 and 25 percent, respectively. Pohl and Van Genderen (1995) integrated data from optical and microwave sensors using image fusion techniques to overcome the cloud cover problem in the tropics. They investigated the geometric aspect of image fusion for topographic map updating. The result shows that the combination of radar with optical data increases the interpretation capabilities and the reliability of the results due to the complementary nature of microwave and optical images. While optical data represent the reflectance of ground cover in visible and near infrared, the radar is very sensitive to the shape, orientation, roughness and moisture content of the illuminated ground objects. Toutin (2000) reported on some aspects of

using mixed radar and visible sensors to generate stereo-pairs that are suitable for stereo-mapping planimetric and elevation features. Quantitative results of mapping and feature extraction from opposite and same side Earth Resource Satellite (ERS)-SAR and SPOT-Pan stereo images were presented in the research. From the stereo-fusion of two types of ERS-SAR/SPOT-Pan pairs, the radiometry of the SPOT-Pan images mainly contributes to the determination of the planimetric features with the quality of its image content; while the geometry of the ERS-SAR image mainly contributes to the determination of the elevation with its high sensitivity to the terrain relief. Canisius and Turral (2003) and Acerbi-Junior *et al.* (2005) presented the results of successful fusion of two multi-spectral sensors with very different spatial and radiometric resolutions: Landsat TM (30 m) and Moderate Resolution Imaging Spectroradiometer (MODIS) (250-500 m). The Landsat TM imagery was used for spatial resolution whereas the MODIS sensor was used to capture most of the vegetation dynamics due to its high temporal resolution. The results showed the potential of the image fusion of medium and high-resolution sensors for land cover mapping.

Natural Hazards Monitoring

The combination of multisensor optical and SAR images also plays an important role in the field of the management of natural hazards monitoring. For example, optical data provide a good basis for the representation of the pre-flood situation in flood monitoring. Then, SAR data acquisition at the time of the flood can be used to identify flood extent and damage. Wang *et al.* (1995) fused ERS-1 SAR with Landsat TM images for flood monitoring in the Netherlands. They demonstrated the SAR imagery plays a key role in environmental and hazard monitoring in areas with continuous cloud cover.

The multi-sensor and time-sequential image fusion approach improves the capability of remote sensing data for natural hazards interpretation. For example, Wiart *et al.* (2000) combined the Japanese Earth Resources Satellite-1 (JERS-1) SAR and Landsat TM imagery to assess the eruptive history of Dubbi volcano, Eritrea. Principal component analysis and optical – SAR fusion were found to be useful to determine the extent of the pumice deposits surrounding the volcano. While the L-band HH polarization (one of the combinations of radar signal transmission and reception: horizontal send, horizontal receive) of the JERS-1 SAR satellite was capable of revealing old lava flows buried below recent pumice deposits. Analysis of both optical and SAR images greatly improved the understanding of the last known eruption of Dubbi volcano and helped to discriminate relative lava flow ages by identifying the pumice deposit. Prakash *et al.* (2001) also used satellite data acquired in three regions of the electromagnetic spectrum (optical, thermal, and microwave), along with field data, to identify the areas affected by coal fires and land subsidence in a coalfield in northwest China. A Landsat TM image was used for the identification of the coalfire areas and the interferometric SAR image was used to identify subsidence areas. Finally, a decision-based fusion was performed to obtain the final fusion product for integrated interpretation.

Geology

Multisensor image fusion is well implemented in the field of geology and is a widely applied technique for geological mapping. Geological features that are not visible in a single image alone may be detected from integrated imagery. In most cases, optical is combined with SAR based on the fact that the datasets complement each other. They introduce information on soil geochemistry, vegetation and land use (from optical image) as well as soil moisture, topography and surface roughness (from SAR image). Jutz and Chorowicz (1993) used an

intensity-hue-saturation (IHS) transform approach to fuse a SPOT panchromatic image and a Landsat TM multispectral image for detailed geological mapping in the Gregory Rift of East Africa. They concluded that the fused image is highly qualified for detailed geological mapping and should be given preference over the respective processing of only TM or SPOT image data because it represents in a synoptic mode the advantages of each system without loss of information. Yesou *et al.* (1994) assessed fracture mapping over a granitic dome in France using different remotely sensed image data such as aerial photographs, SPOT panchromatic and multispectral images, Landsat TM, Seasat, and fused images. The data providing the largest range of scales of observation and the greatest amount of information on geological structures and soil types were the fused image from SPOT panchromatic and Landsat TM images. Ricchetti (2001) fused an ERS-1 SAR image with a Landsat TM image for the geological study of western Aspromonte, Italy. This research demonstrated spectral information provided by the TM image can be effectively combined with texture and pattern data from the radar imagery to produce a fused image in which the geologically relevant information was integrated. Therefore, the fused image can improve the interpretation of lithology boundaries and recognition of structural features.

Existing Techniques for Image Fusion and Limitations

Generally, image rectification and restoration procedures are required for raw remote sensing data to correct the distortions or degradations that stem from the image acquisition process. After having corrected for system errors, optical images must be further radiometrically processed. The type of radiometric correction applied to any given digital image varies widely among sensors. Other things being equal, the radiance measured by any system over a given

object is influenced by such factors as changes in scene illumination, atmospheric condition, viewing geometry, and instrument response characteristics. The need to perform correction for any or all of these influences depends directly upon the particular application (Lillesand *et al.* 2004). In the case of SAR images, speckle reduction is an elementary operation in many applications.

Following the radiometric processing the image data are geometrically corrected. The geocoding plays an essential role in the pixel level image fusion because miss-registration causes artificial colors or features that falsify the following interpretation of the fused image. In some cases, especially if image data of very different spatial resolutions are involved, the resampling of the low-resolution image to the pixel size of the high-resolution image might cause a blocky appearance of the image. Therefore, a smoothing filter can be applied before actually fusing the images (Chavez 1986).

Many image fusion algorithms and software tools have been developed (Pohl and Van Genderen 1998). Conventional methods can be generally classified into four groups: classical IHS transform, PCA, statistical and arithmetic combination, and recently popular wavelet fusion. These techniques have proved promising for fusing radar or SPOT panchromatic images with Landsat TM or other multispectral images (Zhang 2002a).

IHS Transform Method

Digital images are typically displayed as additive color composites using the three primary colors: red, green, and blue (RGB) (Lillesand *et al.* 2004). Figure 2.2 illustrates the RGB components of a typical color display device such as a color monitor. Shown in this figure is the RGB color cube, which is defined by the brightness levels of each of the three primary colors. An alternative to describing colors by their RGB components is the use of the *intensity-hue-*

saturation system. "Intensity" relates to the total brightness of a color on a scale of white to black. "Hue" generally refers to the dominant or average wavelength of light contributing a color. When applied to data displayed on an RGB monitor, hue can be described on a circular scale progressing from red to green to blue and back to red (Figure 2.3). A pixel's hue is determined by the relative proportion of its red, green, and blue inputs. "Saturation" specifies the purity of color relative to gray. Vivid colors are highly saturated, while pale or pastel colors have low saturation.

The IHS transform method can merge a three-band low-resolution multispectral image with a high-resolution panchromatic image (Figure 2.4). First, the multispectral image and the high-resolution panchromatic image are co-registered and the multispectral image is resampled to the resolution of the high-resolution image. Then, the three multispectral bands, R, G, and B, of the low-resolution image are transformed to the IHS color space according to the following equations (Carper *et al.* 1990):

$$\begin{pmatrix} I \\ v_1 \\ v_2 \end{pmatrix} = \begin{pmatrix} \frac{1}{3} & \frac{1}{3} & \frac{1}{3} \\ \frac{1}{\sqrt{6}} & \frac{1}{\sqrt{6}} & \frac{1}{\sqrt{6}} \\ \frac{1}{\sqrt{2}} & -\frac{1}{\sqrt{2}} & 0 \end{pmatrix} \begin{pmatrix} R \\ G \\ B \end{pmatrix} \tag{2.1}$$

$$H = \tan^{-1}\left(\frac{v_2}{v_1}\right), \; S = \sqrt{v_1^2 + v_2^2} \tag{2.2}$$

where I is the intensity, H is the hue, S is the saturation, and v_1, v_2 are intermediate variables.

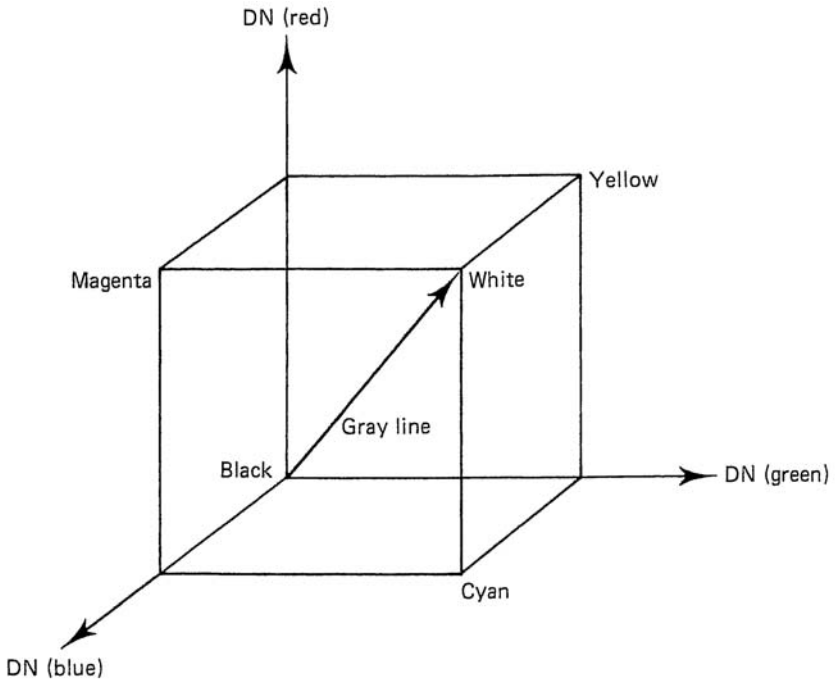

Figure 2.2: The RGB color cube (Schowengerdt 1983).

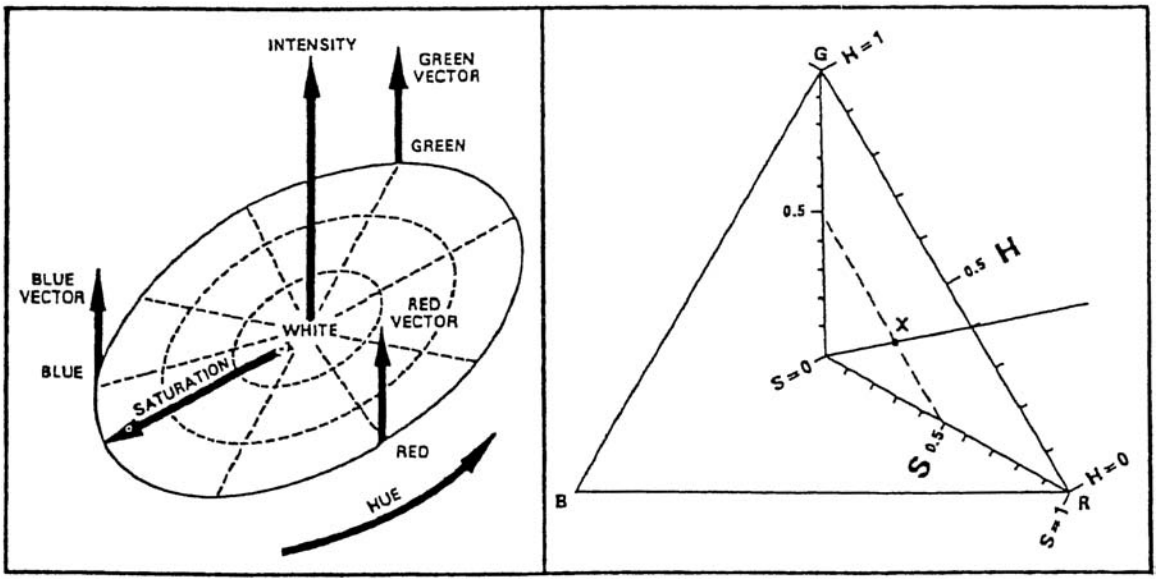

(a) (b)

Figure 2.3: (a) RGB and IHS coordinate systems (Buchanan and Pendergrass 1980);
(b) Simplified IHS representation (Smith 1978 and Haydn *et al.* 1982).

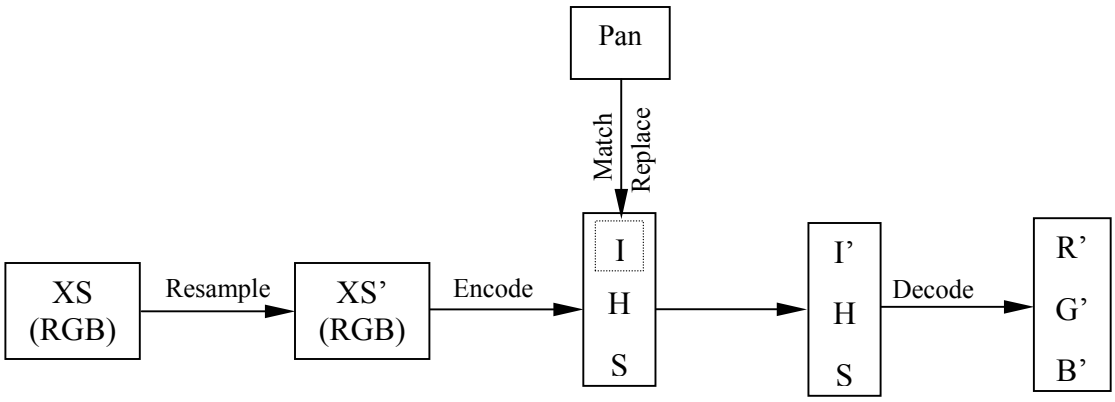

Figure 2.4: Schematic flowchart of the IHS transform method for image fusion.

The high-resolution image is stretched linearly so that it has the same mean and variance properties as those of the intensity image. Then the intensity image is replaced by this stretched high-resolution image. Finally, the new IHS image is transformed back into RGB space to create the fused image (Equation 2.3).

$$\begin{pmatrix} R_{new} \\ G_{new} \\ B_{new} \end{pmatrix} = \begin{pmatrix} 1 & \frac{1}{\sqrt{6}} & \frac{1}{\sqrt{2}} \\ 1 & \frac{1}{\sqrt{6}} & -\frac{1}{2} \\ 1 & -\frac{2}{\sqrt{6}} & 0 \end{pmatrix} \begin{pmatrix} I_{new} \\ v_1 \\ v_2 \end{pmatrix} \qquad (2.3)$$

The IHS transform technique is one of the most widely used image fusion methods in the remote sensing community and is employed as a standard procedure in many commercial packages (Chavez *et al.* 1991, Ehlers 1991, Shettigara 1992, Zhang 1999). Figure 2.5c shows an example of fusing a SPOT panchromatic image with a TM multispectral image of Del Mar, California using the IHS transform method. The original image data are publicly distributed example images of the ERDAS IMAGINE software package.

PCA Method

The PCA method, also known as Karhunen-Loeve transform, is a commonly used tool for analyzing multispectral remote sensing data, especially for image enhancement and data compression. It conducts a linear transformation of the multispectral space to the eigenvector space of the data. Let X represent a $n\times1$ vector of n image bands. Then a principal component transform is

$$Y = A^T X \tag{2.4}$$

where the matrix A is the matrix of eigenvectors, which orthogonalizes the covariance matrix of X such that the covariance matrix of Y is a diagonal matrix, as shown in the following equation (Faust 1989):

$$Cov_y = ACov_x A^T = \begin{pmatrix} \lambda_1 & 0 & 0 & 0 & 0 \\ 0 & \lambda_2 & 0 & 0 & 0 \\ 0 & 0 & . & 0 & 0 \\ 0 & 0 & 0 & . & 0 \\ 0 & 0 & 0 & 0 & \lambda_n \end{pmatrix} \tag{2.5}$$

where $\lambda_1 > \lambda_2 > \ldots > \lambda_n$. The result of the principal components is a set of decorrelated images whose variances of energies are ordered in amplitude.

Using the PCA method to merge a multispectral image of low resolution and a high-resolution image, the multispectal bands (which could be more than 3) are first transformed into the same number of independent principal components. The first principal component image contains the information that is highly correlated to the original multispectral bands used as input to PCA, while spectral information unique to any of the bands is mapped to the other components. Then, similar to the IHS transform method, the first principal component (PC1) is

replaced by the high-resolution image, which is first stretched to have the same mean and variance as PC1. As the last step, the fused image is then derived by performing an inverse PCA transform (Chavez *et al.* 1991, Shettigara 1992, Zhang and Albertz 1997, Zhang 1999) (Figure 2.5d; 2.6).

Arithmetic Combination Techniques

Different arithmetic combinations have been employed for fusing panchromatic and multispectral images. The arithmetic operations of addition, subtraction, multiplication, and division have been combined in different ways to achieve a better fusion effect. The Brovey transform, high pass filtering (HPF), synthetic variable ratio (SVR), and ratio enhancement (RE) techniques are some successful examples for fusing SPOT panchromatic and multispectral images, or a SPOT panchromatic image and a Landsat TM multispectral image.

The Brovey Transform

The Brovey transform uses addition, division, and multiplication for the fusion of three multispectral bands. Its concept can be described with the following formula (ERDAS 2004):

$$band1_{new} = [band1/(band1 + band2 + band3)] \times Pan \qquad (2.6)$$

$$band2_{new} = [band2/(band1 + band2 + band3)] \times Pan \qquad (2.7)$$

$$band3_{new} = [band3/(band1 + band2 + band3)] \times Pan \qquad (2.8)$$

Where *band1*, *band2*, and *band3* are the three bands of the multispectral image, and *Pan* is the panchromatic image with higher spatial resolution.

The Brovey transform was developed to visually increase contrast in the low and high ends of an image histogram (i.e., to provide contrast in shadows, water, and high frequency areas such as urban features). Consequently, the Brovey transform should not be used if preserving the

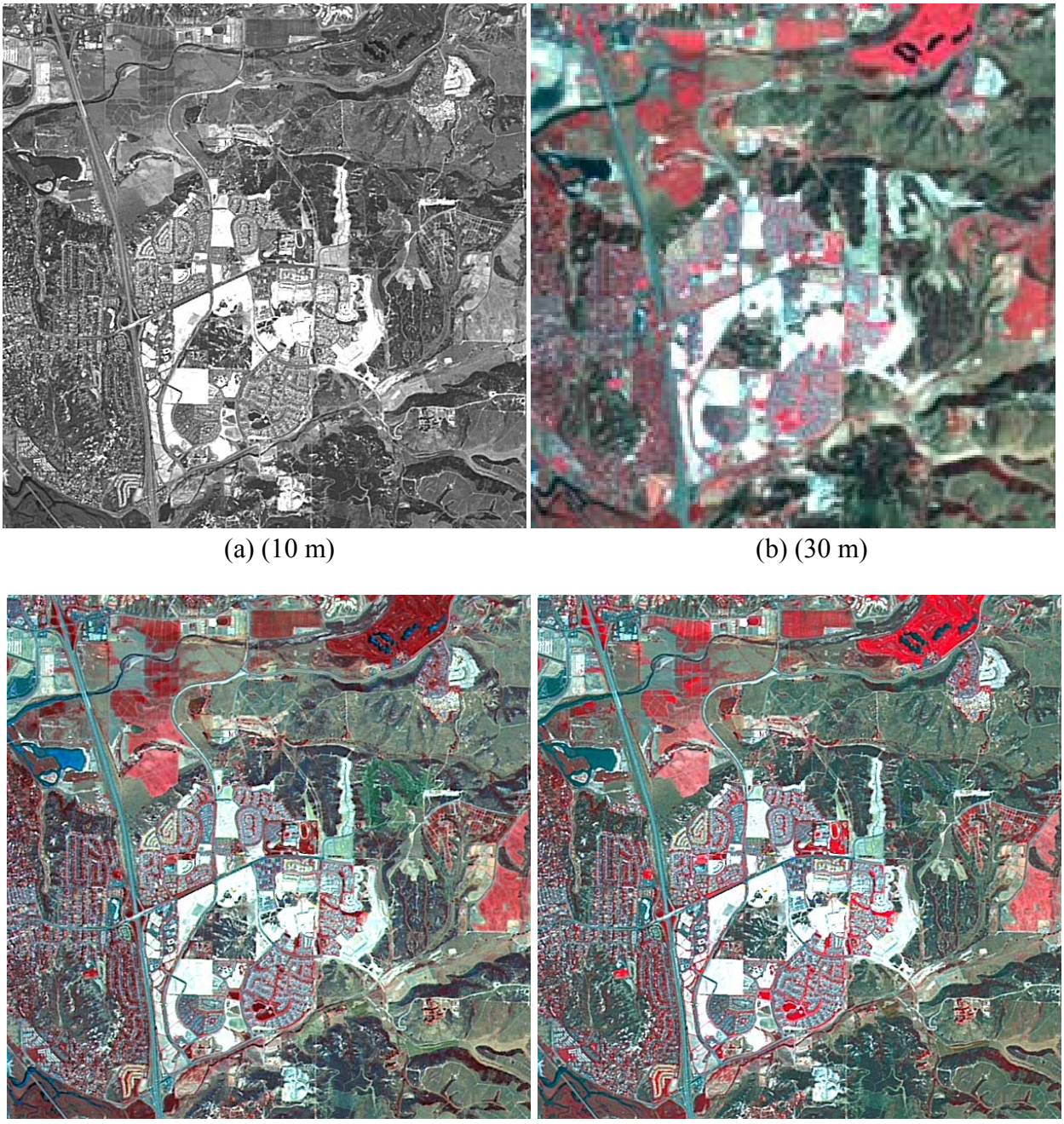

(a) (10 m) (b) (30 m)

(c) (10 m) (d) (10 m)

Figure 2.5: Fusion of SPOT panchromatic and Landsat TM multispectral images of Del Mar, California: (a) SPOT panchromatic image; (b) a color composite of original TM bands 2, 3, and 4; (c) fused image using the IHS transform method; and (d) fused image using the PCA method.

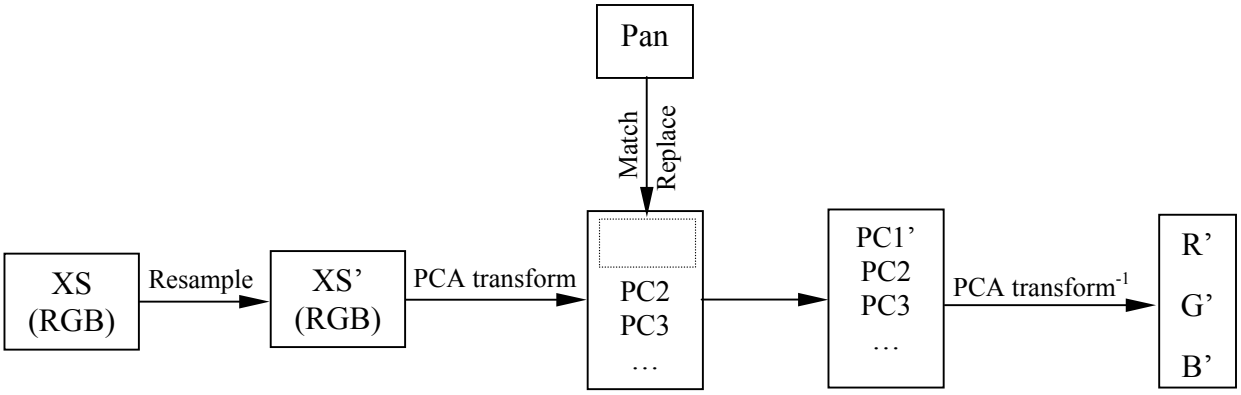

Figure 2.6: Schematic flowchart of the PCA method for image fusion.

original scene radiometry is important. However, it is good for producing RGB images with a high degree of contrast in the low and high ends of the image histogram and for producing visually appealing images. Since the Brovey transform is intended to produce RGB images, only three bands at a time should be fused from the multispectral image, such as bands 1, 2, 3, from a SPOT image or bands 2, 3, 4 from a Landsat TM image. The SVR and RE techniques are similar to the Brovey transform, but involve more sophisticated calculations for the sum image (Cliche *et al.*1985, Welch and Ehlers 1987, Chavez *et al.* 1991, Munechika *et al.*1993, Zhang and Albertz 1997, Zhang 1999).

High Pass Filtering (HPF)

High Pass Filtering (HPF) is another approach to enhance the spatial resolution of multispectral image. The basic idea of HPF is to add the spatial information to the spectral information: high pass filtering in combination with band addition. In this method a high pass filter is applied to the high spatial resolution image. The results of the small high pass filter contain the high-frequency component/information that is related mostly to spatial information. The results then are added pixel by pixel to the lower spatial resolution, but high spectral

resolution image. This allows the higher resolution image to add equally to each of the lower resolution images using the simple pixel addition method without distorting the spectral balance. The HPF method was first discussed by Schowengerdt (1983) as a procedure to extrapolate edge information from a high-resolution band to lower spatial resolution bands. This method also was previously used by Chavez (1986) to merge TM data with digitized National High Altitude Program (NHAP) data and Chavez and Bowell (1988) to merge TM and SPOT panchromatic data.

Wavelet Technique

As a powerful mathematical tool, wavelet transform was developed in the field of signal and image processing (Petrosian and Meyer 2001). More recently, wavelets have started playing a role in image fusion. The original principle of wavelet image fusion is to get the best resolution without altering the spectral contents of the image. More clearly, this principle is based on multiresolution analysis provided by the wavelet transforms (Mallat 1989). Wavelet transforms are capable of decomposing a digital image into a set of multiresolution images, accompanied by wavelet coefficients for each resolution level. The wavelet coefficients for each level contain the spatial differences between two successive resolution levels. The general steps of wavelet-based fusion are: (1) decomposition of a high resolution panchromatic image into a set of low resolution panchromatic images with wavelet coefficients for each level, (2) replacement of a low resolution panchromatic band with a multispectral band at the same resolution level, and (3) performance of a reverse wavelet transform to convert the decomposed and replaced panchromatic set back to the original panchromatic resolution level. The replacement and reverse transform are done three times, once for each multispectral band. Previous work on wavelet transform for data fusion can be found in Li *et al.* (1995), Rockinger *et al.* (1996), Yocky (1996),

Zhou *et al.* (1998), Couloigner *et al.* (1998), Nunez *et al*. (1999), Ranchin and Wald (2000), and Gomez *et al*. (2001).

Limitations of Existing Techniques

Problems and limitations associated with the available fusion techniques have been reported by many studies (Chavez *et al.* 1991, Pellemans *et al.* 1993, Wald *et al.* 1997, Van Der Meer 1997, Zhang 2002a). According to these studies, the most significant problem is the color distortion of fused images (i.e., the spectral difference between the original multispectral and fused images). In image fusion, it is desirable to minimize the color distortion since this ensures that features separable in the original multispectral image are still separable in the fused image (Chavez *et al.* 1991). To reduce the distortion, the suggested strategies for IHS transform method are, for example, matching the panchromatic image to the intensity component before the replacement, stretching the hue and saturation components before the reverse transform, or stretching individual I, H or S components with respect to individual datasets. In PCA image fusion, dominant spatial information and weak color information are often problems. The reason is that the first principal component being replaced usually contains a maximum variance. Such replacement maximizes the effect of the panchromatic image in the fused image. Suggested solutions include stretching the principal components to give a spherical distribution, or discarding the first principal component.

With the Brovey transform, it is necessary to select only three bands. In general, the pixel gray values are smaller than those of other fusion techniques. The color distortion is obvious and varies depending on the band combinations being fused. With the SVR and RE techniques, the color effect of the fused image is generally better than the Brovey Transform, but a suitable preprocessing is necessary before the fusion (Zhang 2002b). With wavelet-based fusion, the

color distortion can be reduced to a certain extent, but the color does not appear smoothly integrated into the spatial features. Other disadvantages also have been reported, for example, the loss of spectral content of small objects (Yocky 1996, Ranchin and Wald 2000).

When the existing fusion techniques are applied to the fusion of new generation high-resolution satellite images such as Ikonos and QuickBird images, the color distortions are much more significant (Zhang 2002a). Figure 2.7 shows the results of fusing Ikonos panchromatic and multispectral images using IHS transform method in two different areas – Fredericton, Canada and San Diego, USA. The same IHS algorithm and fusion parameters were applied to the two image sets. It can be clearly seen that (1) the color of the fused image is distorted from their original color, and (2) the color distortion tended in different ways for different image sets (Zhang 2002a). For example, in Fredericton image set, the color of the vegetated areas, marked as *A* in Figure 2.7, changed from green in the original multispectral image to light green in the fused image. However, the color of the grass filed of the Stadium, marked as *B* in Figure 2.7, may change from green to light blue in the San Diego image set.

A major reason for this color distortion is the change of the panchromatic spectral range (Zhang 2002a). Different from the SPOT panchromatic channel, the wavelength of Ikonos and QuickBird panchromatic channels is extended from visible to near infrared range (Table 2.1). This change makes the gray value relationship of an Ikonos or QuickBird panchromatic image significantly different from that of a SPOT panchromatic image (Figure 2.8). For example,

Table 2.1: Spectral Ranges of Different Panchromatic Images

Satellite sensor	Spectral range (μm)
SPOT	0.51 – 0.73
Ikonos	0.45 – 0.90
QuickBird	0.45 – 0.90

vegetated areas (marked as *E* in Figure 2.8) in the SPOT panchromatic image (Figure 2.8*a*) appear darker than pavement areas (marked as *F* in Figure 2.8). However, they may appear brighter than pavement areas in an Ikonos panchromatic image (Figure 2.8*b*) because of the influence of near infrared content. Therefore, conventional fusion algorithms, which have been successful for the fusion of SPOT panchromatic and other multispectral images, cannot effectively fulfill the fusion of these new images.

Figure 2.8*c* show the intensity image transformed from Ikonos multispectral bands 1, 2, and 3. The grey value difference between the Ikonos Pan and the intensity image is more significant than that between the SPOT Pan and the intensity image. When the intensity image is replaced by a significantly different image – Ikonos Pan, the IHS fusion will, of course, lead to a significant color distortion. In the opposite, if the intensity is replaced by a panchromatic image like the SPOT Pan, the color distortion of the IHS fusion would be much smaller. Similarly, the first component from the PCA method is also significantly different from the original Ikonos Pan image, which causes the color distortion in the fused image (Zhang 2002a).

With more high-resolution commercial satellite images (e.g., Ikonos, QuickBird, and OrbView-3) now available for public and private geospatial information communities, advanced image fusion techniques for these image data are needed to fully extend their potential. In this study, the fast Fourier transform (FFT) filtering and wavelet transform are considered to enhance the existing IHS transform method for fusing these new images. The following two sections will continue to review the Fourier and wavelet transforms and their applications in image processing.

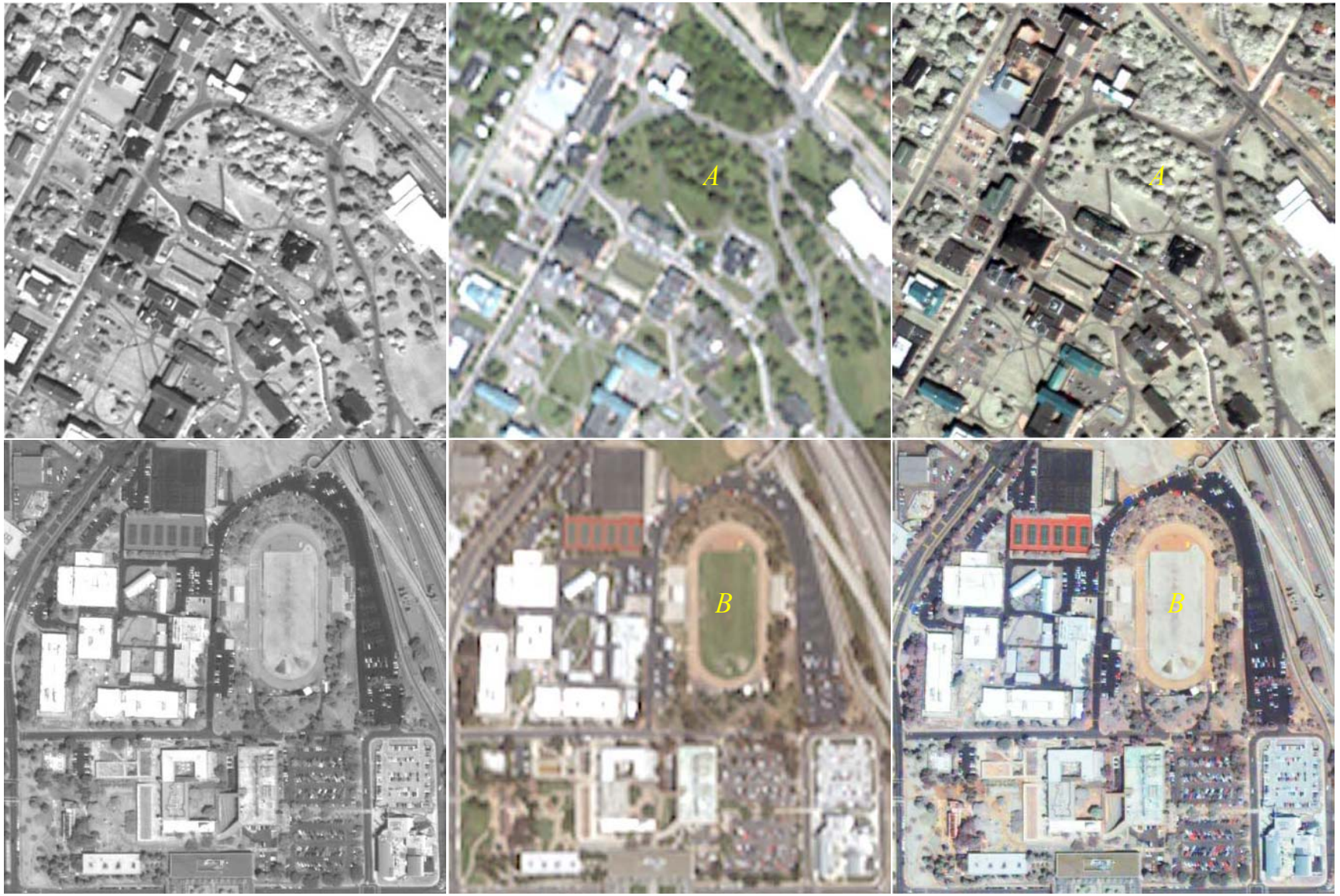

Figure 2.7: Different color distortions of the same IHS fusion algorithm and parameters. From left to right: original Ikonos Pan image with 1-m resolution, original Ikonos natural color images with 4-m resolution, and IHS fusion results. Top: Fredericton, Canada. Bottom: San Diego, the USA (Zhang 2002a).

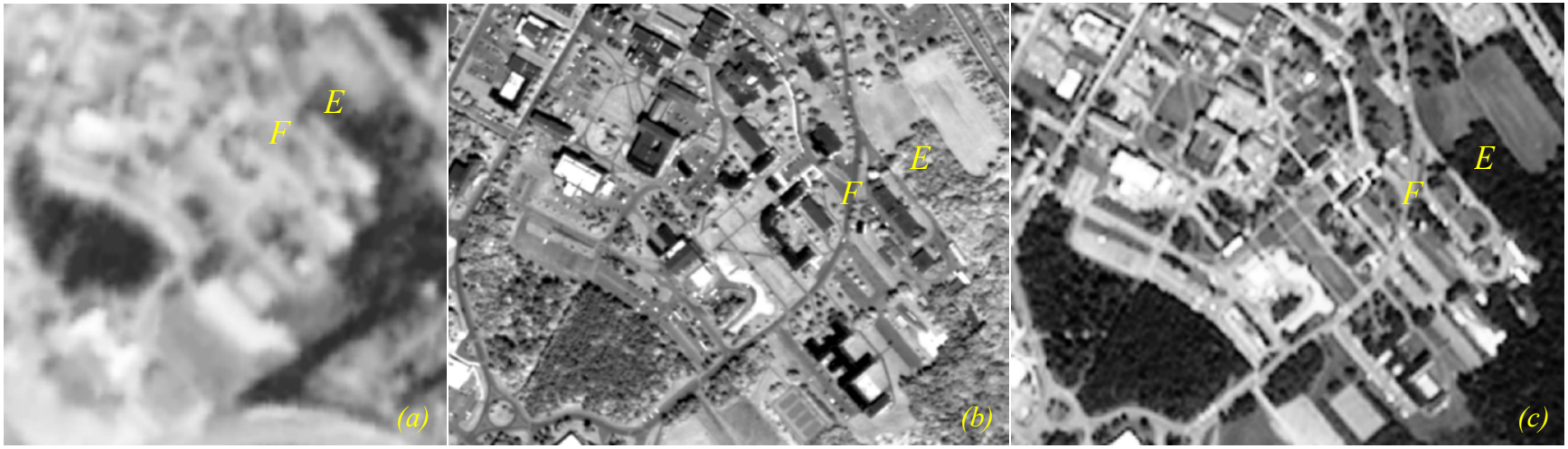

Figure 2.8: Comparison of gray value differences among (a) SPOT Pan, (b) Ikonos Pan (middle), and (c) Ikonos intensity (right) (Zhang 2002a).

Fourier Transform and Image Filtering in the Frequency Domain

The Frequency Domain

Spatial feature manipulations usually are implemented in the spatial domain – the (x, y) coordinate space of images. An alternative coordinate space that can be used for image analysis is the frequency domain. In this approach, an image is separated into its various spatial frequency components through application of a mathematical operation known as the Fourier transform. The Fourier transform of a two-dimensional function is shown mathematically as the following equation (Mai 1999):

$$H(u,v) = \int_{-\infty}^{\infty}\int_{-\infty}^{\infty} h(x,y)e^{-j2\pi(ux+vy)}dxdy \qquad (2.9)$$

Where $$j = \sqrt{-1} \quad and \quad e^{\pm jx} = \cos(x) \pm j\sin(x) \qquad (2.10)$$

The Fourier transform deals with complex numbers. It is not immediately obvious what the real and imaginary parts represent. Another way to represent the data is with its sign (phase) and magnitude. The magnitude is expressed as:

$$|H(u,v)| = \sqrt{R^2(u,v) + I^2(u,v)} \qquad (2.11)$$

and phase as

$$\theta(u,v) + \tan^{-1}\left[\frac{I(u,v)}{R(u,v)}\right] \qquad (2.12)$$

where *R (u,v)* is the real part and *I (u,v)* is the imaginary. The magnitude is the amplitude of sine and cosine waves in the Fourier transform formula. As expected, 0 is the phase of the sine and cosine waves. This information, along with the frequency, allows us to fully specify the sine and cosine components of an image.

After an image is separated into its component spatial frequencies, it is possible to display these values in a two-dimensional scatter plot known as a *Fourier spectrum.* Figure 2.9 illustrates a digital image and its Fourier spectrum. Since the frequency is dependent on the pixel location in the transform, the lower frequencies in the scene are plotted at the center of the spectrum and progressively higher frequencies are plotted outward. Features trending horizontally in the original image result in vertical components in the Fourier spectrum; features aligned vertically in the original image result in horizontal components in the Fourier spectrum (Lillesand *et al.* 2004). If the Fourier spectrum of an image is known, it is also possible to transform the image data from the frequency domain back to the spatial domain. This is done with an inverse Fourier transform:

$$h(x,y) = \int_{-\infty}^{\infty}\int_{-\infty}^{\infty} H(u,v)e^{-j2\pi(ux+vy)}dudv \tag{2.13}$$

Hence, the Fourier spectrum of an image can be used to assist in a number of image processing operations.

Discrete Fourier Transform (DTF) and Fast Fourier Transform (FFT)

The discrete Fourier transform (DFT) is a special case of the continuous Fourier transform. Since a digital image is represented by a finite number of discrete samples (i.e., pixels) that compose the image, Fourier analysis of images requires the DFT. The formula to compute the DFT on an $M \times N$ size image is

$$H(u,v) = \sum_{x=0}^{M-1}\sum_{y=0}^{N-1} h(x,y)e^{-j2\pi 2\pi(ux+vy/N)} \tag{2.14}$$

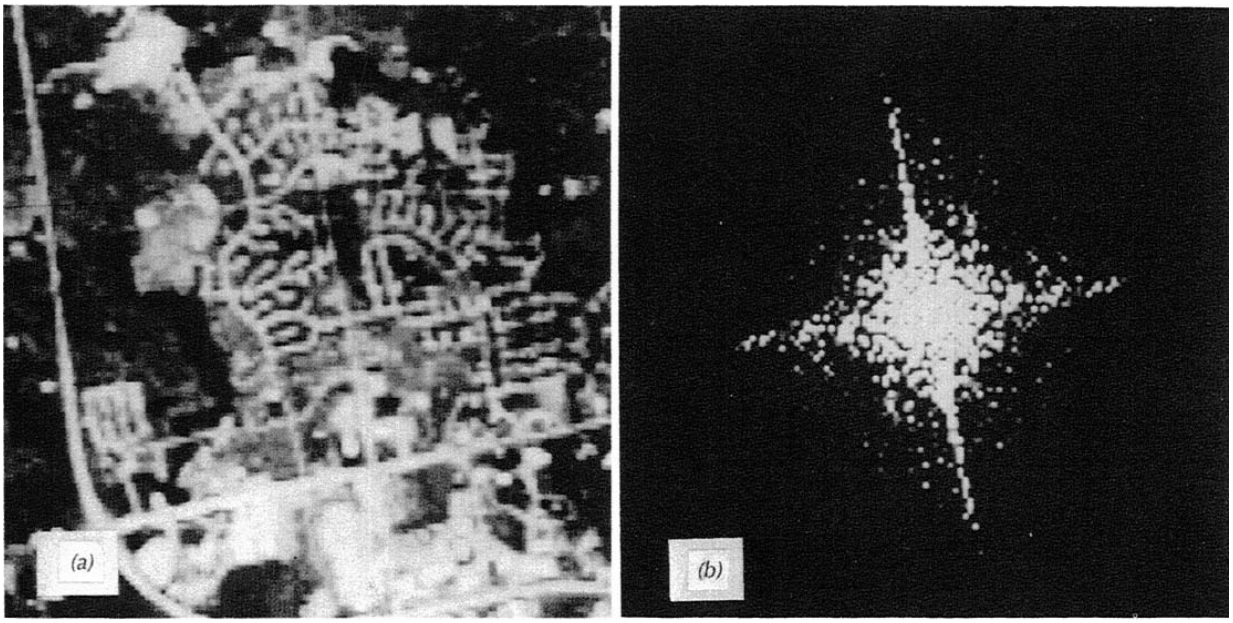

Figure 2.9: Application of Fourier transform: (a) original image; (b) Fourier spectrum of (a) (Lillesand *et al.* 2004).

The formula to transform the image back to the spatial domain is

$$h(x,y) = \frac{1}{MN}\sum_{x=0}^{M-1}\sum_{y=0}^{N-1} H(u,v)e^{j2\pi(ux/M+vy/N)} \tag{2.15}$$

There is a ringing problem known as Gibb's phenomenon for DFT because of the finite samples (Smith 1999). To reduce this problem, a windowing function (sometimes called window weighting functions) can be multiplied to the data before the Fourier transform is performed.

The FFT is a computationally efficient implementation of the DFT. It reduces the number of complex multiplications from N^2 for DFT to the order of $N\log_2 N$. This savings is substantial especially for image processing.

Image Filtering in the Frequency Domain

One common motive to generate image frequency data is to filter the data. The process of image filtering in the frequency domain is quite simple: (1) to transform image data to the frequency domain via the FFT; (2) to multiply the image spectrum with some filtering mask; and (3) to transform the spectrum back to the spatial domain. The two methods of creating a filtering mask are to transform a convolution mask from the spatial domain to the frequency domain and to calculate a mask within the frequency domain. The reason for doing the filtering in the frequency domain is generally because it is computationally faster to perform two two-dimensional FFT and a filter multiplication than to perform a convolution in the spatial domain. This is particularly so as the filter size increases (Bourke 1998).

There are many types of filters, but most are a derivation or combination of four basic types: low pass, high pass, bandpass, and bandstop or notch filter. A low pass filter passes low frequencies while attenuating the higher frequencies. A high pass filter attenuates the low frequencies and passes higher frequencies. Bandpass filters allow a specific band of frequencies to pass unaltered. Bandstop filters attenuate only a specific band of frequencies. Figure 2.10 illustrates an example of low pass and high pass filtering in the frequency domain (Lillesand *et al.* 2004). In Figure 2.10*a*, a circular high frequency blocking filter has been applied to the Fourier spectrum shown previously in Figure 2.9*b*. Note that the filtered image shown in Figure 2.10*b* is a low pass filtered version of the original image shown in Figure 2.9*a*. Figures 2.10*c* and *d* illustrate the application of a circular low frequency blocking filter *(c)* to produce a high pass filtered enhancement *(d)*. Because of its computational efficiency, the FFT has been widely used in image enhancement (filtering) and restoration (i.e., noise removal) (Brigham 1988, Lillesand *et al.* 2004, Morita 1995).

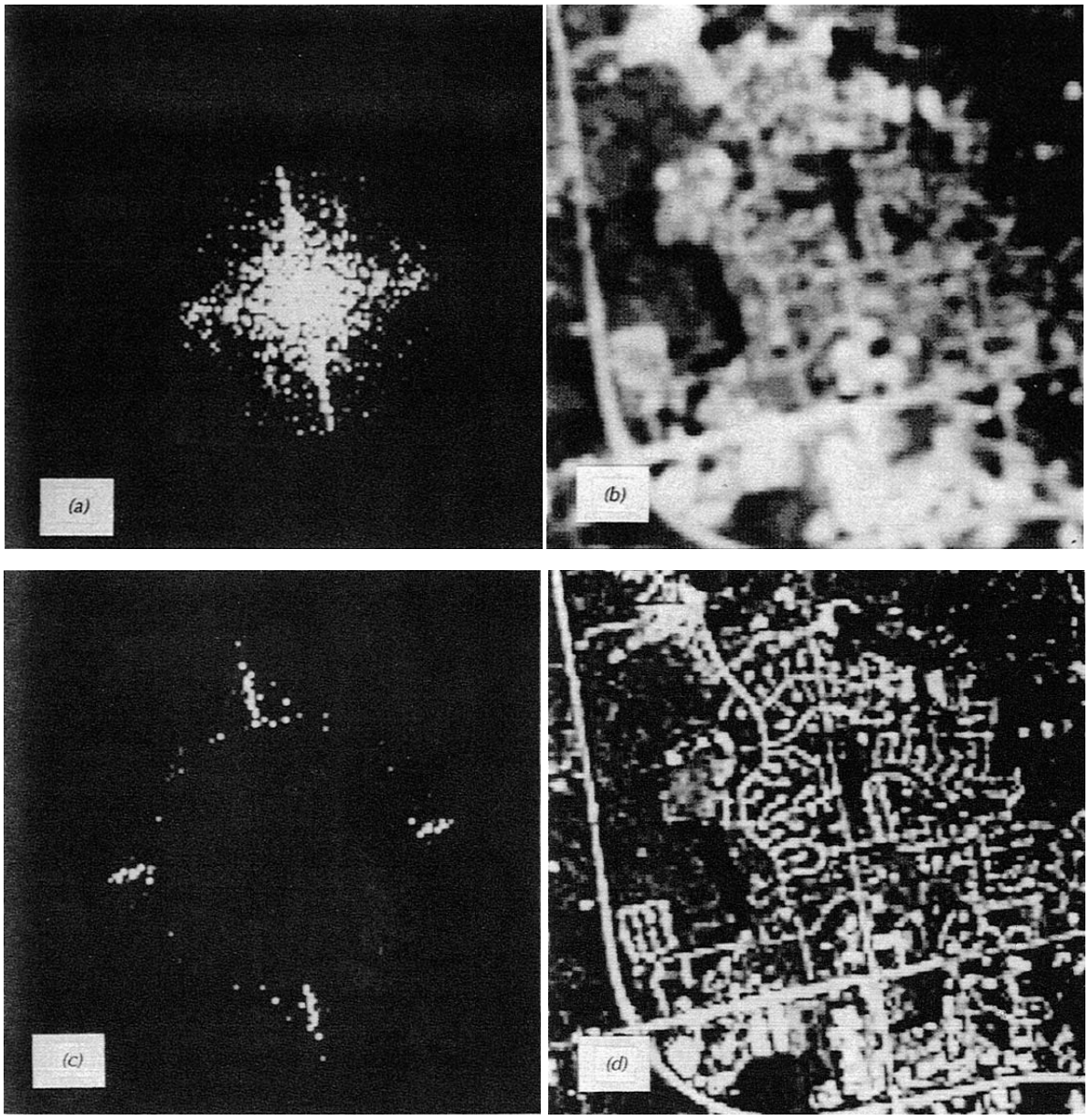

Figure 2.10: Image filtering in the frequency domain: (a) high frequency blocking filter; (b) inverse transform of (a); (c) low frequency blocking filter; (d) inverse transform of (c) (Lillesand *et al.* 2004).

Wavelet Transform for Image Processing

Wavelet Theory

Wavelet-based image reduction is similar to the Fourier transform analysis. In the Fourier transform, long continuous (sine and cosine) waves are used as the basis. The wavelet transform uses short, discrete "wavelet" instead of a long wave. Thus the new transform is much more local (Strang and Nguyen 1997). In image processing terms, the wavelet can be parameterized as a finite size moving window. While the Fourier transform gives an idea of the frequency content in an image, the wavelet representation is an intermediate representation between the Fourier and the spatial representation, and it can provide good localization in both frequency and space domains (Nunez *et al.* 1999). The wavelet transform of a distribution *f (x)* can be expressed by the following equation (Mallat 1989):

$$W(f)(a,b) = |a|^{-\frac{1}{2}} \int_{-\infty}^{+\infty} f(x)\Psi\left(\frac{t-b}{a}\right)dx \qquad (2.16)$$

where *a* and *b* are scaling and translational parameters, respectively. Each base function $\Psi\left(\frac{x-b}{a}\right)dx$ is a scaled and translated version of a function Ψ called *mother wavelet*. These base functions are $\int \Psi\left(\frac{x-b}{a}\right) = 0$. A key element of using wavelets is selection of the mother wavelet, which is the basic waveform to be used to represent the image. The input signal (or image) is broken down into successively smaller multiples of this basis. If the wavelet coefficients are known, it is possible to reconstruct the original signal (or image) without loss of information.

This is done with an inverse wavelet transform:

$$f(x) = \frac{1}{C_\Psi} \int_{-\infty}^{+\infty} \int_{-\infty}^{+\infty} W(f)(a,b) \Psi_{a,b}(x) \frac{dadb}{a^2} \qquad (2.17)$$

where C_Ψ is the admissibility condition of the mother wavelet.

In practice the coefficients of the discrete high pass filter are of more interest than the wavelets themselves. The wavelets are rarely even calculated (Shensa 1992). In image processing, instead of deeply involving mathematical decomposition, relatively rapid processing kernels (moving windows) are used to approximate the waveform decomposition. Once selected, the wavelets are applied to the input image recursively via a pyramid algorithm or filter bank. This is commonly implemented as a cascading series of high-pass and low-pass filters, based on the mother wavelet, applied sequentially to the low-pass image of the previous recursion. After filtering at any level, the low-pass image (commonly termed the "approximation" image) is passed to the next finer filtering in the filter bank. The high-pass images (termed "horizontal", "vertical", and "diagonal") are retained for later image reconstruction. In practice, three or four recursions are sufficient (ERDAS 2004).

Two-Dimensional Discrete Wavelet Transform (DWT)

A two-dimensional Discrete Wavelet Transform (DWT) of an image yields four components (ERDAS 2004): (1) approximation coefficients W_φ, (2) horizontal coefficients W_ψ^H - variation along the columns, (3) vertical coefficients W_ψ^V - variation along the rows, and (4) diagonal coefficients W_ψ^D - variation along the diagonals. As shown in Figure 2.11, symbols h_φ and h_ψ are, respectively, the low-pass and high-pass wavelet filters used for decomposition. The rows of the image are convolved with the low-pass and high-pass filters and the result is down-

sampled along the columns. This yields two sub-images whose horizontal resolutions are reduced by a factor of 2. The high-pass or detailed coefficients characterize the image's high frequency information with vertical orientation, while the low-pass component contains its low frequency, vertical information. Both sub-images are again filtered column-wise with the same low-pass and high-pass filters and down-sampled along rows. Thus, for each input image, we have four sub-images each reduced by a factor of 4 compared to the original image: W_{φ}, W_{ψ}^{H}, W_{ψ}^{V}, and W_{ψ}^{D}.

Similarly, for the inverse DWT, the reduced components of the input images are passed as input to the low-pass and high-pass reconstruction filters $\tilde{h}_{\varphi}$ and $\tilde{h}_{\psi}$ (different from those

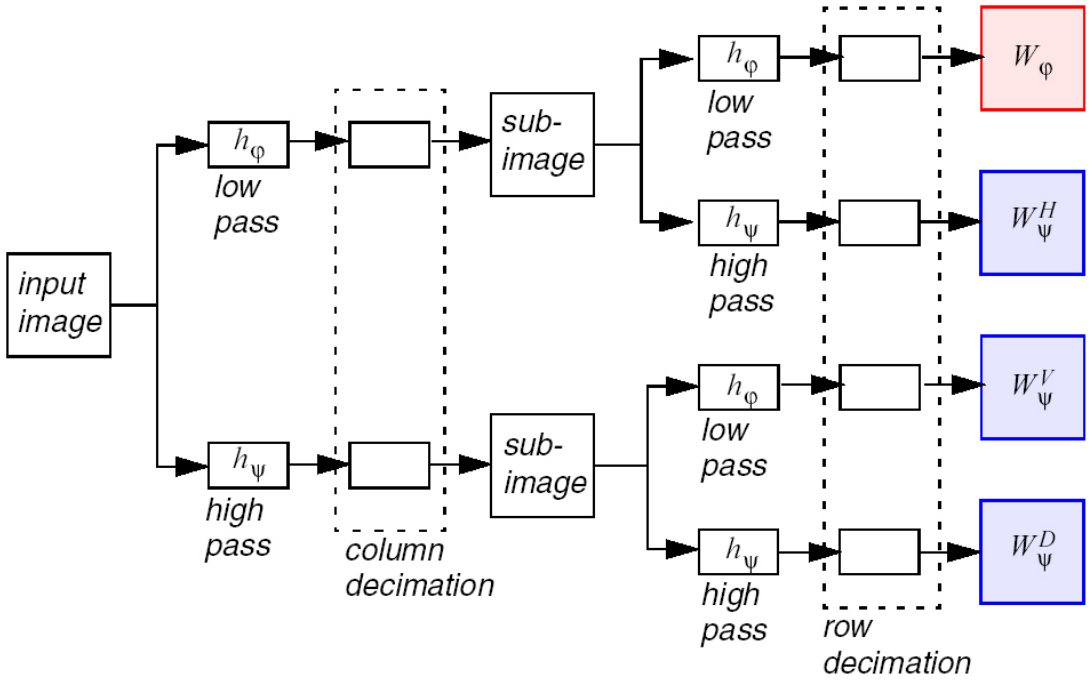

Figure 2.11: Schematic diagram of the discrete wavelet transform (ERDAS 2004).

used for decomposition) as shown in Figure 2.12. The sequence of steps is the opposite of that in the DWT. The sub-images are up-sampled along rows and convolved with low-pass and high-pass filters by columns. These intermediate outputs are concatenated, up-sampled along columns and then filtered along rows and finally concatenated to yield the output image.

Figure 2.13 shows an example of two-dimensional DWT applied on a SPOT panchromatic image. The original image is a subset of one example image provided by the ERDAS IMAGINE software package. Wavelet transforms are proving useful in a wide variety of image processing applications, including image enhancement, compression, and fusion (Meyer 1993, Louis *et al.* 1997, Rao and Bopardikar 1998, Pohl and Van Genderen 1998).

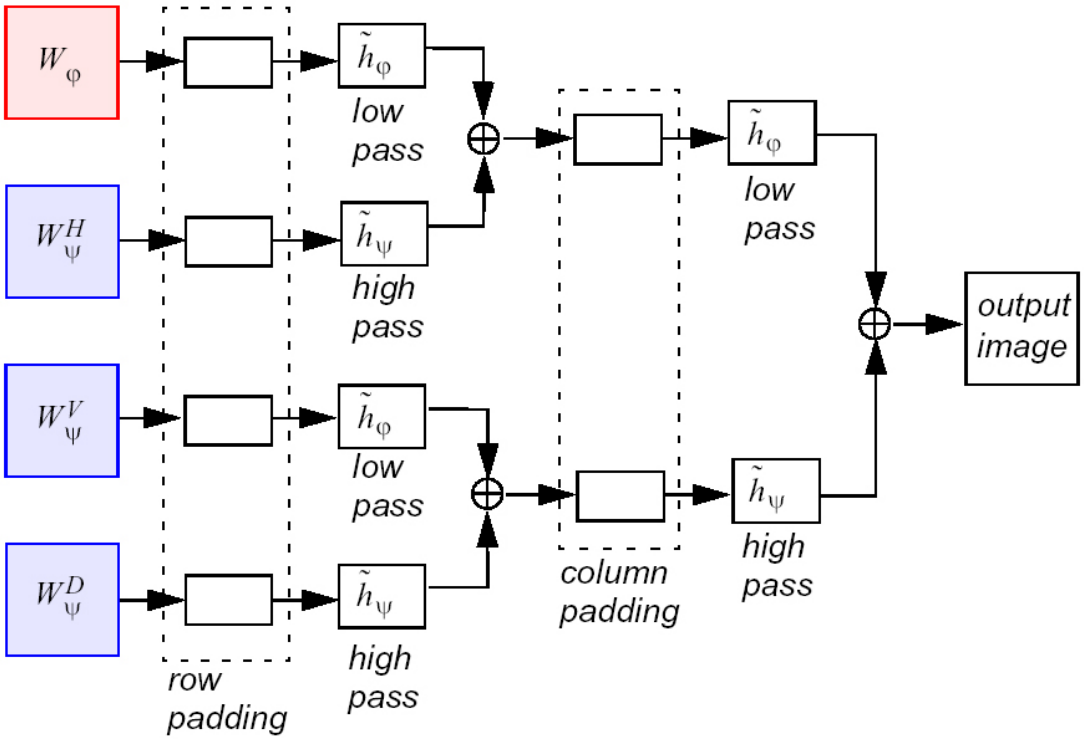

Figure 2.12: Schematic diagram of the inverse discrete wavelet transform (ERDAS 2004).

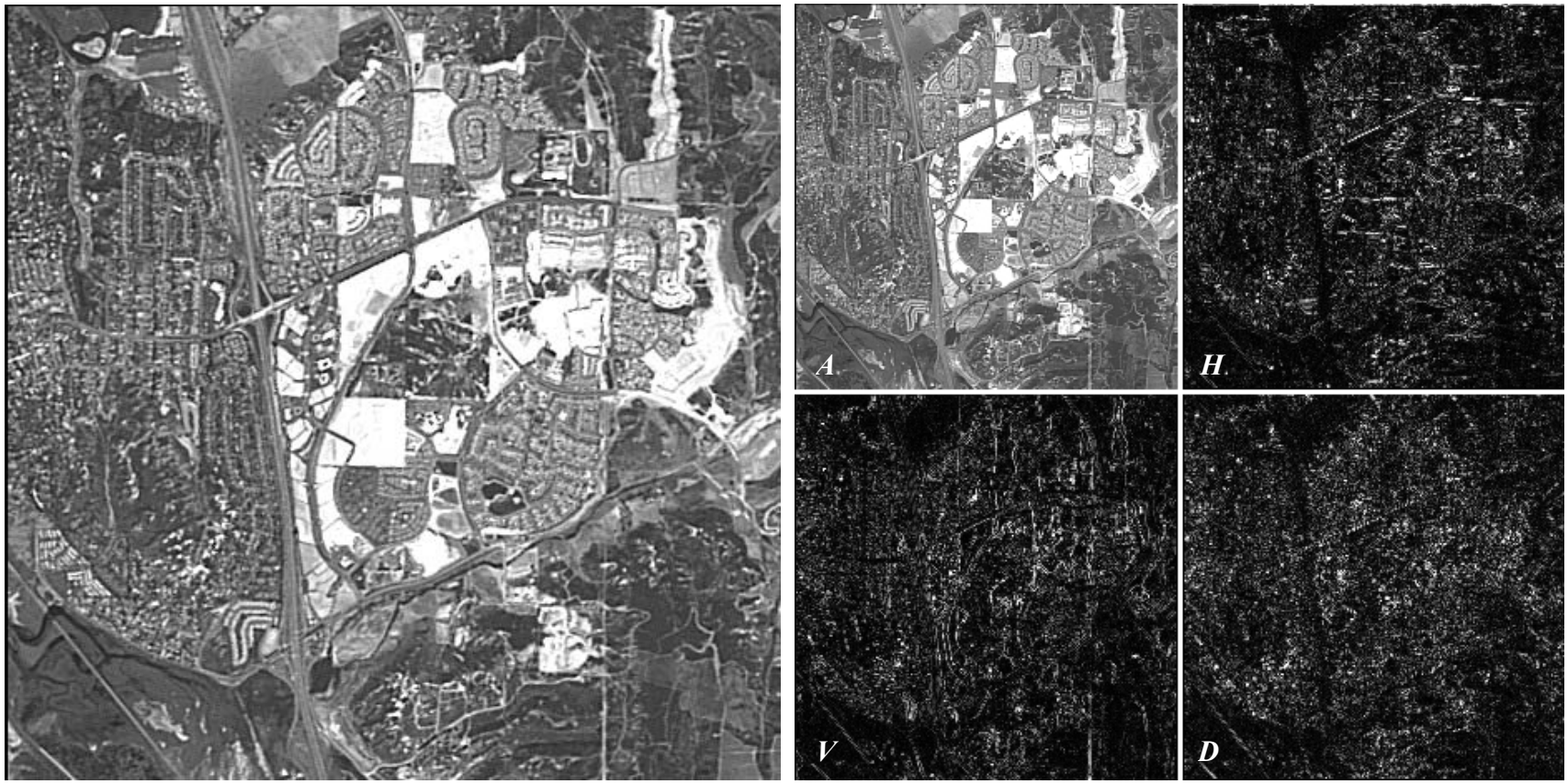

(a) (b)

Figure 2.13: An example of the two-dimensional DWT: (a) original SPOT panchromatic image; (b) four components obtained from the decomposition: *A* – approximation coefficients, *H* – horizontal coefficients, *V* – vertical coefficients, and *D* – diagonal coefficients.

Conclusions for Literature Review

Remote sensing data from commercial sensors offer the geospatial communities important new sources of timely and accurate spatial information that can augment data provided by public-sector remote sensing system. Because of the complementary benefits of image fusion, it is still a popular tool to interpret image data. According to Schulman (2002), as the sensor market heats up to some estimates, there will be a huge market and big profit in fusion, exploitation, and dissemination of sensor data in ways that improve knowledge creation.

The purpose of this review was to provide a better understanding of image fusion techniques by first examining the existing image fusion techniques, followed by exploring their limitations for fusing new generation high-resolution commercial satellite images. From this review, it is clear that advanced image fusion techniques are needed for fusing these high-resolution commercial satellite images. In the next chapter, two advanced image processing techniques – FFT and wavelet transform, will be employed to enhance the existing IHS transform method for fusing commercial high-resolution images such as Ikonos and QuickBird data. Chapter 4 will examine how the resolution ratio of input images affects the quality of the fused image.

References

Acerbi-Junior, F.W., R. Zurita Milla, J.G.P.W. Clevers, M.E. Schaepman, and M. Wachowicz, 2005. MODIS and Landsat TM image fusion using the SIFuLAP method for mapping the Brazilian savannas (Cerrado), *Proceedings of 25th EARSeL Symposium-Global Developments in Environmental Earth Observation from Space*, Porto, Portugal, 6-11 June 2005, CD-ROM.

Ackerman, F., 1995. Sensor- and data-integration – the new challenge, In *Integrated Sensor Orientation: Theory*, *Algorithms and Systems*, edited by Colimina, I. and J. Navarro (Heidelberg: Wichmann), pp. 2 – 10.

Bourke, P., 1998. Image filtering in the frequency domain, URL: http://astronomy.swin.edu.au/~pbourke/other/imagefilter/, Victoria, Australia (last date accessed, 29 September 2005).

Brigham, E.O., 1988. *The Fast Fourier Transform and its Applications*, Englewood Cliffs, NJ, Prentice Hall, 448 p.

Buchanan, M.D. and R. Pendergrass, 1980. Digital image processing: can intensity, hue, and saturation replace red, green and blue? *Electro-Optical System Design*, Vol. 12, No. 3, pp. 29 – 36.

Canisius, F.X.J. and H. Turral, 2003. Fusion technique to extract detail information from moderate resolution data for global scale image map production, *Proceedings of the 30th International Symposium on Remote Sensing of Environment – Information for Risk Management and Sustainable Development*, November 10-14, 2003 Honolulu, Hawaii.

Carper, W.J., T.M. Lillesand, and R.W. Kiefer, 1990. The use of Intensity-Hue-Saturation transformations for merging SPOT Panchromatic and multispectral image data, *Photogrammetric Engineering and Remote Sensing*, Vol. 56, No. 4, pp. 459 – 467.

Chavez, P.S., 1986. Digital merging of Landsat TM and digitized NHAP data for 1:24 000 scale image mapping, *Photogrammetric Engineering and Remote Sensing*, Vol. 52, No. 10, pp. 1637 – 1646.

Chavez, P.S. and J. Bowell, 1988. Comparison of the spectral information content of Landsat Thematic Mapper and SPOT for three different sites in the Phoenix, Arizona Region, *Photogrammetric Engineering and Remote Sensing*, Vol. 54, No. 12, pp. 1699 – 1708.

Chavez, P.S., S.C. Sides, and J.A. Anderson, 1991. Comparison of three different methods to merge multiresolution and multispectral data: TM & SPOT pan, *Photogrammetric Engineering and Remote Sensing*, Vol. 57, No. 3, pp. 295 – 303.

Cliche, G., F. Bonn, and P. Teillet, 1985. Integration of the SPOT Pan channel into its multispectral mode for image sharpness enhancement, *Photogrammetric Engineering and Remote Sensing*, Vol. 51, No. 3, pp. 311 – 316.

Couloigner, I., T. Ranchin, V. Valtonen, and L. Wald, 1998. Benefit of the future SPOT-5 and of data fusion to urban roads mapping, *International Journal of Remote Sensing*, Vol. 19, No. 8, pp. 1519 – 1532.

Donnay, J.P., M.J. Barnsley, and P. Longley, 2001. Remote Sensing and Urban Analysis, edited by Donnay, J.P., M.J. Barnsley, and P.A. Longley, Chapter 1, London, New York: Taylor & Francis.

Ehlers, M., 1991. Multisensor image fusion techniques in remote sensing, *ISPRS Journal of Photogrammetry and Remote Sensing*, Vol. 46, pp. 19 – 30.

ERDAS *Imagine Field Guide*, 2004, Leica Geosystems, LLC, Atlanta, GA.

Faust, N.L., 1989. Image enhancement, In: Kent, A. and J.G. Williams (editors), *Encyclopedia of Computer Science and Technology*, Vol. 20, Supplement 5, Marcel Deker Inc., New York.
Gomez, B.R., A. Jazaeri, and M. Kafatos, 2001. Wavelet-based hyperspectral and multispectral image fusion, *2001 SPIE's OE/Aerospace Sensing, Geo-Spatial Image and Data Exploitation II*, Orlando, April 16 – 20, 2001.

Hall, D.L. and J. Llinas, 1997. An introduction to multisensor data fusion, In *Proceedings of* the *IEEE*, Vol. 85, No. 1, pp. 6 – 23.

Haydn, R., G.W. Dalke, and J. Henkel, 1982. Application of the IHS color transform to the processing of multisensor data and image enhancement, *Proceedings of the International Symposium on Remote Sensing of Arid and Semiarid Lands*, Cario, Egypt, pp. 599 – 616.

Jones, J.G., R.W. Thmomas, and P.G. Earwicker, 1991. Multiresolution analysis of remotely imagery, *International Journal of Remote Sensing*, Vol. 12, No. 1, pp. 107 – 124.

Jutz, S.L. and J. Chorowicz, 1993. Geological mapping and detection of oblique extension structures in the Kenyan Rift Valley with a SPOT/Landsat-TM datamerge, *International Journal of Remote Sensing*, Vol. 14, No. 9, pp. 1677 – 1688.

Li, H., B.S. Manjunath, and S.K. Mitra, 1995. Multisensor image fusion using the wavelet transform, *Graphical Models and Image Processing*, Vol. 57, No. 3, pp. 235 – 245.

Lillesand, T.M., R.W. Kiefer, and J.W. Chipman, 2004. *Remote Sensing and Image Interpretation*, 5th edition, John Wiley & Sons, 763 p.

Louis, A.K., P. Maass, and A. Rieder, 1997. *Wavelets: Theory and Applications*, Chichester, New York: Wiley.

Mai, L.C., 1999. Introduction to computer vision and image processing, URL: http://www.netnam.vn/unescocourse/computervision/comp_frm.htm, Hanoi, Vietnam (last date accessed: 29 September 2005).

Mallat, S.G., 1989. A theory for multiresolution signal decomposition: The wavelet representation, *IEEE Transactions on Pattern Analysis and Machine Intelligence*, Vol. 11, No. 7, pp. 674 – 693.

Meyer Y., 1993. *Wavelets, Algorithms and Applications*, Philadelphia, PA: SIAM, 1993.

Morita, K., 1995. *Applied Fourier Transform*, Tokyo, Japan: Ohmsha; Burke, VA: IOS Press.

Munechika, C.K., J.S. Warnick, C. Salvaggio, and J.R. Schott, 1993. Resolution enhancement of multispectral image data improve classification accuracy, *Photogrammetric Engineering and Remote Sensing*, Vol. 59, No. 1, pp. 67 – 72.

Nunez, J., X. Otazu, O. Fors, A. Prades, V. Pala, and R. Arbiol, 1999. Multiresolution-based image fusion with adaptive wavelet decomposition, *IEEE Transactions on Geoscience and Remote Sensing*, Vol. 37, No. 3, pp. 1204 – 1211.

Pellemans, A.H.J.M., R.W.L. Jordans, and R. Allewijn, 1993. Merging multispectral and panchromatic SPOT images with respect to the radiometric properties of the sensor, *Photogrammetric Engineering and Remote Sensing*, Vol. 59, No. 1, pp. 81 – 87.

Petrosian, A.A. and F.G. Meyer, 2001. *Wavelets in Signal and Image Analysis: From Theory to Practice*, Kluwer Academic Publishers.

Pohl, C. and J.L. Van Genderen, 1995. Image fusion of microwave and optical remote sensing data for map updating in the Tropics, *Image and Signal Processing for Remote Sensing, Proceedings EUROPT O '95, Paris, France, 25-29 September 1995*, SPIE Vol. 2579, pp. 2 – 10.

Pohl, C. and J.L. Van Genderen, 1998. Multisensor image fusion in remote sensing: concepts, methods and applications, *International Journal of Remote Sensing*, Vol. 19, No. 5, pp. 823 – 854.

Prakash, A., E.J. Fielding, R. Gens, J.L. Van Genderen, and D.L. Evans, 2001. Data fusion for investigating land subsidence and coal fire hazards in a coal mining area, *International Journal of Remote Sensing*, Vol. 22, No. 6, pp. 921 – 932.

Ranchin, T., L. Wald, and M. Mangolini, 1996. The ARSIS method: a general solution for improving spatial resolution of images by the means of sensor fusion, *Fusion of Earth Data*, *Proceedings EARSeL Conference, Cannes, France, 6 – 8 February 1996* (Paris: European Space Agency).

Ranchin, T. and L. Wald, 2000. Fusion of high spatial and spectral resolution images: the ARSIS concept and its implementation, *Photogrammetric Engineering and Remote Sensing*, Vol. 66, No. 1, pp. 49 – 61.

Rao, R.M. and A.S. Bopardikar, 1998. *Wavelet Transforms: Introduction to Theory and Applications*, Reading, MA: Addison-Wesley.

Ricchetti, E., 2001. Visible-infrared and radar imagery fusion for geological application: a new approach using DEM and sun-illumination model, *International Journal of Remote Sensing*, Vol. 22, No. 11, pp. 2219 – 2230.

Rockinger, O., 1996. Pixel - level fusion of image sequences using wavelet frames, In: *Proceedings of the 16th Leeds Applied Shape Research workshop*, Leeds University Press.

Rogers, R.H. and L. Wood, 1990. The history and status of merging multiple sensor data: an overview, *Technical Papers 1990, ACSM – ASPRS Annual Convention, Image Processing and Remote Sensing,* Vol. 4, pp. 352 – 360.

Schulman, A., 2002. Who will capitalize on the next major market opportunity? *Imaging Notes*, July/August, 2002.

Schowengerdt, R.A., 1983. *Techniques for Image Processing and Classification in Remote Sensing*, Academic, New York, 249p.

Shensa, M., 1992. The discrete wavelet transform: wedding the A Trous and Mallat algorithms, *IEEE Transactions on Signal Processing*, Vol. 40, No. 10, pp. 2464 – 2482.

Shettigara, V.K., 1992. A generalized component substitution technique for spatial enhancement of multispectral images using a higher resolution data set, *Photogrammetric Engineering and Remote Sensing*, Vol. 58, No. 5, pp. 561 – 567.

Smith, A.R., 1978. Color gamut transform pairs, *Computer Graphics*, Vo. 12, No. 3, pp. 12 – 18.

Smith, W.S., 1999. *The Scientist and Engineer's Guide to Digital Signal Processing*, California Technical Publishing, second Edition.

Strang, G. and T. Nguyen, 1997. *Wavelets and Filter Banks*, Wellesley-Cambridge Press.

Toutin, T., 2000. Stereo-mapping with SPOT-P and ERS-1 SAR images, *International Journal of Remote Sensing*, Vol. 21, No. 8, pp. 1657 – 1674.

Van Der Meer, F., 1997. What does multisensor image fusion add in terms of information content for visual interpretation? *International Journal of Remote Sensing*, Vol. 18, No. 2, pp. 445 – 452.

Van Genderen, J.L. and C. Pohl, 1994. Image fusion: Issues, techniques and applications, *Intelligent Image Fusion, Proceedings EARSeL Workshop, Strasbourg, France, 11 September 1994*, edited by Van Genderen J.L. and V. Cappellini, pp. 8 – 26.

Wald, L., T. Ranchin, and M. Magolini, 1997. Fusion of satellite images of different spatial resolutions: assessing the quality of resulting images, *Photogrammetric Engineering and Remote Sensing*, Vol. 63 No. 6, pp. 69 – 699.

Wald, L., 1999. Some terms of reference in data fusion, *IEEE Transactions on Geoscience and Remote Sensing*, Vol. 37, No. 3, pp. 1190 – 1193.

Wang, Y., B.N. Koopmans, and C. Pohl, 1995. The 1995 flood in The Netherlands monitored from space – a multi-sensor approach, *International Journal of Remote Sensing*, Vol. 16, No. 15, pp. 2735 – 2739.

Welch, R., 1982. Spatial resolution requirements for urban studies, *International Journal of Remote Sensing*, Vol. 3, No. 2, pp. 139 – 146.

Welch, R. and M. Ehlers, 1987. Merging multiresolution SPOT HRV and Landsat TM data, *Photogrammetric Engineering and Remote Sensing*, Vol. 53, No. 3, pp. 301 – 303.

Welch, R. and M. Ehlers, 1988. Cartographic feature extraction from integrated SIR-B and Landsat TM images, *International Journal of Remote Sensing*, Vol. 9, No. 5, pp. 873 – 889.

Wiart, P.A.M., C. Oppenheimer, and P. Francis, 2000. Eruptive history of Dubbi volcano, northeast Afar (Eritrea), revealed by optical and SAR image interpretation, *International Journal of Remote Sensing*, Vol. 21, No. 5, pp. 911 – 936.

Yesou, H., Y. Besnus, and J. Rolet, 1994. Perception of a geological body using multiple source remotely-sensed data – relative influence of the spectral content and the spatial resolution, *International Journal of Remote Sensing*, Vol. 15, No. 12, pp. 2495 – 2510.

Yocky, D.A., 1996. Multiresolution wavelet decomposition image merger of Landsat Thematic Mapper and SPOT panchromatic data, *Photogrammetric Engineering and Remote Sensing*, Vol. 62, No. 9, pp. 1067 – 1074.

Zhang, Y. and J. Albertz, 1997. Comparison of four different methods to merge multisensor and multiresolution satellite data for the purpose of mapping, *Proceedings of the ISPRS Joint Workshop 'Sensors and Mapping from Space' of Working Groups I/1*, *I/3 and IV/ 4*, *Hannover*, *Germany*, *29 September – 2 October 1997*, pp. 275 – 287.

Zhang, Y., 1999. A new merging method and its spectral and spatial effects, *International Journal of Remote Sensing*, Vol. 20, No. 10, pp. 2003 – 2014.

Zhang, Y., 2002a. Problems in the fusion of commercial high-resolution satellite images as well as Landsat 7 images and initial solutions, *Interational Archives of Photogrammetry and Remote Sensing (IAPRS)*, Vol. 14, Part 4, Ottawa, July 2002.

Zhang, Y., 2002b. Automatic image fusion: A new sharpening technique for IKONOS multispectral images, *GIM International*, Vol. 16, No. 5, pp. 54 – 57.

Zhang, Y. and R. Wang, 2004. Multi-resolution and multi-spectral image fusion for urban object extraction, *XXth ISPRS Congress, Commission 3*, Istanbul, 2004.

Zhou, J., D.L. Civco, and J.A. Silander, 1998. A wavelet transform method to merge Landsat TM and SPOT panchromatic data, *International Journal of Remote Sensing*, Vol. 19, No. 4, pp. 743 – 757.

CHAPTER 3

ENHANCED IHS TRANSFORM METHODS FOR FUSING COMMERCIAL HIGH-RESOLUTION SATELLITE IMAGES[1]

[1] Ling, Y., M. Ehlers, E.L. Usery, and M. Madden. To be submitted to *ISPRS Journal of Photogrammetry and Remote Sensing*.

Abstract

Existing image fusion techniques such as the intensity-hue-saturation (IHS) transform and principal components analysis (PCA) methods may not be optimal for fusing the new generation commercial high-resolution satellite images such as Ikonos and QuickBird. One problem in fusing images is color distortion, which causes visual changes as well as spectral differences between the original and fused images. In this paper, two enhanced IHS methods, a fast Fourier transform (FFT)-enhanced IHS method and a wavelet-enhanced IHS method, are developed for fusing new generation commercial high-resolution satellite images. The FFT-enhanced IHS transform method combines a standard IHS transform with FFT filtering of both the panchromatic image and the intensity component of the original multispectral image. Similarly, the wavelet-enhanced IHS transform method uses a partial replacement based on a wavelet-based technique in which high-resolution wavelet coefficients of the panchromatic image are fused with the multispectral image. Ikonos and QuickBird data are used to assess these enhanced IHS transform methods. The two enhanced IHS transform methods may improve upon the traditional IHS transform and the PCA methods in preserving visual, spectral and spatial information.

Introduction

During sensor design, for the purpose of receiving enough energy at a specific dwelling time, a panchromatic band covering a broad range of the wavelength spectrum, and several multispectral bands each covering a narrow spectral range are specified at different spatial resolutions. Most Earth observation satellite systems, therefore, provide two types of image data: a panchromatic image with high-spatial resolution and a multispectral image with relatively

lower spatial resolution, but higher spectral resolution. Image fusion, a technique of merging two images to create a new image, is capable of effectively combining the high-spatial information from the panchromatic data and the multispectral information from the multispectral data into a single image. In this way, image fusion can extend the application potential of remote sensing images since many applications require both high spatial and high spectral resolution.

A variety of image fusion methods have been developed in the past two decades (e.g., Cliche *et al.* 1985, Price 1987, Welch and Ehlers 1987, Chavez *et al.* 1991, Ehlers 1991, Shettigara 1992, Yesou *et al.* 1993, Zhang 1999, Zhang 2002). The two traditional methods are the intensity-hue-saturation (IHS) transform and principal components analysis (PCA) methods. They are also the most commonly used algorithms by the remote sensing community (Zhang 1999, Tu *et al.* 2001). However, the fused image from these two methods usually has a notable deviation in visual appearance and in spectral values from the original image. These deviations, called color distortion, affect further interpretation, especially when the wavelength range of a panchromatic image does not correspond to that of the employed multispectral image. Multi-temporal images are another problem since the panchromatic and multispectral data are often taken at different seasons or years. On the other hand, most of these methods have been used in the fusion of radar or SPOT panchromatic image data with Landsat Thematic Mapper (TM) and other types of multispectral images.

In the fusion of the new generation satellite images such as Landsat Enhanced Thematic Mapper Plus (ETM+), Ikonos, and QuickBird, the wavelength extension of the panchromatic band into the near infrared may result in color distortion in the fused image when the traditional image fusion techniques are employed (Zhang 2002). Consequently, the objective of this study is to enhance the standard IHS transform method using advanced image analysis techniques

including fast Fourier transform filtering and wavelet transforms. Instead of using a total replacement of the intensity component as in the standard IHS transform method, the new methods replace the high frequency part of the intensity component only.

Study Area and Image Data

The study area is located in Camp Lejeune (34° 35' N latitude, 77° 18' W longitude), southeastern North Carolina (Figure 3.1). Camp Lejeune lies in the coastal plain with relative flat terrain (typically relief is less than 25 m) and the climate is mild to moderate with average of annual temperature of 17.2 °C and precipitation of 1372 mm (Onslow County 2005).

Two datasets for the Camp Lejeune study area are used in this research. One is a QuickBird dataset over a built-up area with urban features, marked as *A* in Figure 3.1. This area includes a populated subdivision with houses and associated trees, lawns, and shrubs. Roads in this area wind through dense vegetation and are partially obscured. Also, included in this area is a large golf course with greens, trees, and sand traps. The populated subdivision is adjacent to a retail and commercial section of the city including roads, buildings, parking lots, and other features that reflect the concrete and asphalt of an urban area. The other dataset is an Ikonos image over a complex region, marked as *B* in Figure 3.1, with sea, land, and air features. The land area in this image contains different types of vegetation including mixed conifer and deciduous forests, grassy areas, and some vegetated wetlands.

Each dataset contains a panchromatic band and three multispectral bands (Table 3.1). The images are spatially registered to the Universal Transverse Mercator (UTM) coordinate system on the WGS 84 datum.

Table 3.1: Image Data Used in the Study

Image data	Spectral bandwidth (μm)	Spatial resolution (m)	Acquisition date
Ikonos Pan	0.45 – 0.90	1	2/5/2000
Ikonos XS (Bands 2, 3, 4)	Band 2: 0.51 – 0.60 Band 3: 0.63 – 0.70 Band 4: 0.76 – 0.85	4	8/27/2001
QuickBird Pan	0.45 – 0.90	0.61	3/3/2003
QuickBird XS (Bands 2, 3, 4)	Band 2: 0.52 – 0.60 Band 3: 0.63 – 0.69 Band 4: 0.76 – 0.85	2.44	3/24/2003

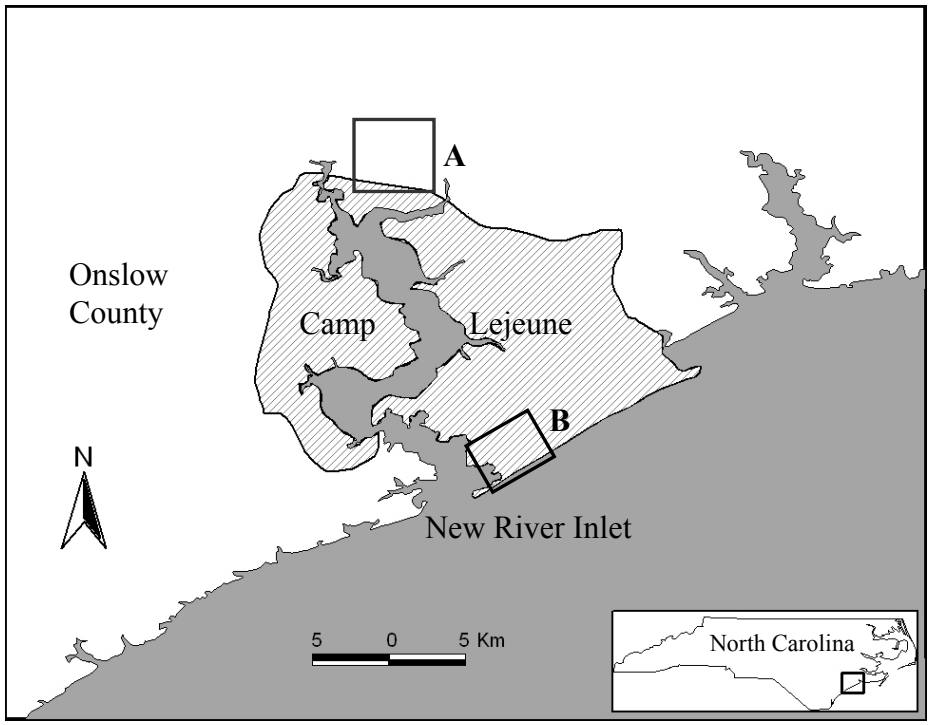

Figure 3.1: Camp Lejeune study area, North Carolina.

Methodology

The Standard IHS Transform Method for Image Fusion

The IHS color transform can effectively convert a multispectral image from standard *red-green-blue* (RGB) color space to IHS color space. Among the advantages of IHS transform operations is the ability to vary each IHS component independently, without affecting the others (Lillesand *et al.* 2004). This property may be used for the fusion of multi-sensor images. The basic steps of IHS fusion are: (1) transform the input multispectral image from RGB to IHS color space. The mathematical context is expressed by Equations 3.1 and 3.2. I relates the intensity, while v_1, v_2 are intermediate variables, and H and S stand for hue and saturation, respectively (Carper *et al.* 1990); (2) replace the intensity component by a panchromatic image with a higher spatial resolution; and (3) transform the replaced intensity component, together with original hue and saturation components, back to RGB color space to create the fused image (Equation 3.3) (Carper *et al.* 1990). To enhance the operation of this process and better retain the spectral

$$\begin{pmatrix} I \\ v_1 \\ v_2 \end{pmatrix} = \begin{pmatrix} \frac{1}{3} & \frac{1}{3} & \frac{1}{3} \\ \frac{1}{\sqrt{6}} & \frac{1}{\sqrt{6}} & \frac{1}{\sqrt{6}} \\ \frac{1}{\sqrt{2}} & -\frac{1}{\sqrt{2}} & 0 \end{pmatrix} \begin{pmatrix} R \\ G \\ B \end{pmatrix} \tag{3.1}$$

$$H = \tan^{-1}\left(\frac{v_2}{v_1}\right),\ S = \sqrt{v_1^2 + v_2^2} \tag{3.2}$$

$$\begin{pmatrix} R_{new} \\ G_{new} \\ B_{new} \end{pmatrix} = \begin{pmatrix} 1 & \frac{1}{\sqrt{6}} & \frac{1}{\sqrt{2}} \\ 1 & \frac{1}{\sqrt{6}} & -\frac{1}{2} \\ 1 & -\frac{2}{\sqrt{6}} & 0 \end{pmatrix} \begin{pmatrix} I_{new} \\ v_1 \\ v_2 \end{pmatrix} \tag{3.3}$$

information of the original image, one can use a Fourier or wavelet transform to decompose the intensity component and replace only a part of it. The application of these methods is discussed below.

FFT-Enhanced IHS Transform Method

Fourier Transform and Image Filtering in the Frequency Domain

The Fourier transform is an important image processing tool that is used to decompose an image into its sine and cosine components. The Fourier transform of a two-dimensional function can be expressed as the following equations (Gonzales and Woods 1992):

$$H(u,v) = \int_{-\infty}^{\infty}\int_{-\infty}^{\infty} h(x,y)e^{-j2\pi(ux+vy)}dxdy \qquad (3.4)$$

Where $$j = \sqrt{-1} \quad and \quad e^{\pm jx} = \cos(x) \pm j\sin(x) \qquad (3.5)$$

The output of the transformation represents the image in the Fourier or frequency domain, while the input image is the spatial domain equivalent. In the Fourier domain image, each point represents a particular frequency contained in the spatial domain image. If a Fourier domain image is known, it can be transformed back to the spatial domain using an inverse Fourier transform (Gonzales and Woods 1992):

$$h(x,y) = \int_{-\infty}^{\infty}\int_{-\infty}^{\infty} H(u,v)e^{-j2\pi(ux+vy)}dudv \qquad (3.6)$$

Since digital image processing involves a finite number of discrete samples (i.e., pixels), a modified form of the Fourier transform, known as the discrete Fourier transform (DFT), is used in Fourier image analysis. A computationally efficient implementation of the DFT is the fast Fourier transform (FFT).

Image filtering in the frequency domain has been widely used in image processing since convolution by multiplication in the frequency domain is computationally faster than conventional convolution in the spatial domain, especially as the filter size increases (Smith 1999). Also, once in the frequency domain, it is easier to analyze the "frequency content" of the image and design an appropriate low-pass or high-pass filter (Jain 1989).

Image Fusion with FFT-Enhanced IHS Transform Method

The basic idea behind the FFT-enhanced IHS transform method is to modify the input high-resolution panchromatic image so it looks more like the intensity component of the input multispectral image. Instead of using a total replacement of the intensity component, this method uses a partial replacement based on FFT filtering.

In the FFT-enhanced IHS transform method, the multispectral image is first transformed using the IHS transform. A frequency domain analysis is used to select a low-pass filter for the original intensity component and a high-pass filter for the panchromatic image. The idea is to substitute the high frequency part of the intensity component with that from the panchromatic image. Both the low-pass and high-pass filters should be complementary, i.e., the high frequency part removed from the intensity component should be the only part left in the panchromatic image. After the replacement of the high frequency information from the panchromatic image, the new intensity component, together with the original hue and saturation components, is transformed back to RGB color space to obtain the fused image (Figure 3.2). The procedure of image fusion using the FFT-enhanced IHS transform method is summarized in Table 3.2.

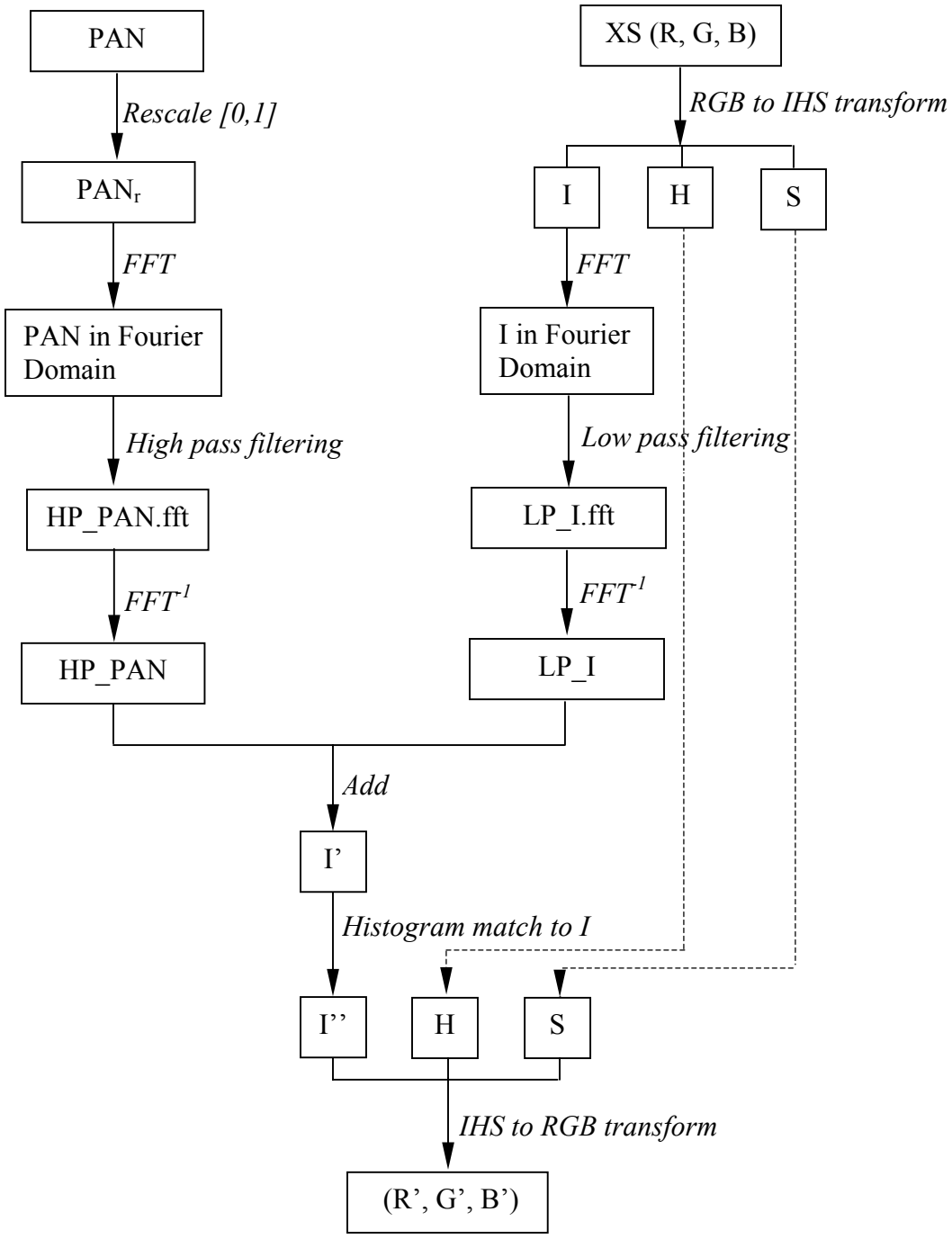

Figure 3.2: Schematic diagram for the FFT-enhanced IHS transform method.

Table 3.2: The Procedure of Image Fusion Using the FFT-Enhanced IHS Transform Method.

1	Register all images to the panchromatic image and resample to the highest resolution (e.g. Ikonos 1-m, QuickBird 0.61-m) using cubic convolution.
2	Transform the resampled multispectral image from the RGB to IHS color space to obtain the intensity (*I*), hue (*H*), and saturation (*S*) components.
3	Low-pass filtering of the intensity component, *I*, by designing an appropriate filter in the Fourier domain.
4	High-pass filtering of the panchromatic image in the Fourier domain.
5	Add the high frequency filtered panchromatic image to the low frequency filtered intensity component, *I*, for the new intensity component, *I'*.
6	Match *I'* to the original *I* to obtain a new intensity component, *I''*.
7	Perform an IHS to RGB transform on *I''*, together with the original hue (*H*) and saturation (*S*) components, to create the fused image.

Wavelet-Enhanced IHS Transform Method

The Wavelet Transform

The wavelet transform enables an input signal or image to be decomposed on the basis of a series of elementary functions – known as *wavelets*. These are generated by dilations and translations of a single function, known as the 'mother' wavelet (Mallat 1989):

$$\Psi_{a,b} = |a|^{-\frac{1}{2}} \Psi\left(\frac{x-b}{a}\right) \tag{3.7}$$

where *a* and *b* are scaling and translational parameters, respectively. In the one-dimensional case, the continuous wavelet transform of a function *f (x)* is given by Equation 3.8.

$$W(f)(a,b) = |a|^{-\frac{1}{2}} \int_{-\infty}^{+\infty} f(x)\Psi\left(\frac{x-b}{a}\right)dx \tag{3.8}$$

Each base function $\Psi\left(\frac{x-b}{a}\right)dx$ is a scaled and translated version of a function Ψ (i.e., mother wavelet). These base functions are $\int \Psi\left(\frac{t-b}{a}\right) = 0$. The computation of the wavelet transform for each scale and each location of a signal (or image) provides a local representation of this signal (or image). The process can be inverted so that the original signal (or image) can be

reconstructed exactly (i.e., without loss) from the wavelet coefficients using the following equation:

$$f(x) = \frac{1}{C_\Psi} \int_{-\infty}^{+\infty} \int_{-\infty}^{+\infty} W(f)(a,b) \Psi_{a,b}(x) \frac{dadb}{a^2} \tag{3.9}$$

where C_Ψ is the admissibility condition of the mother wavelet.

Discrete Wavelet Transform for Image Fusion

A 2-dimensional discrete wavelet transform (DWT) decomposes an image into the coarser resolution representation that consists of the low frequency approximation information (i.e., approximation coefficients W_φ,) and the high frequency detail information (i.e., horizontal coefficients W_ψ^H, vertical coefficients W_ψ^V, and diagonal coefficients W_ψ^D) (Mallat 1989). During the decomposition, the resolution decreases exponentially at the base of 2. Therefore, the size of the decomposed images is one fourth of the original size and the resolution is one half of the original image (Figure 3.3). The reconstruction of the original image can be achieved through the inverse discrete wavelet transform (IDWT).

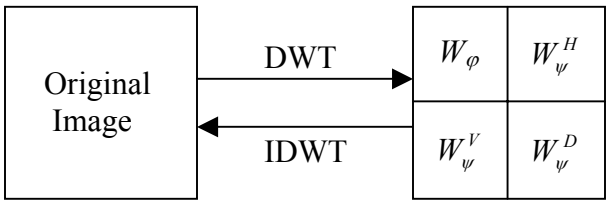

Figure 3.3: Diagram of one level wavelet transform.

Recently, wavelet-based techniques become popular in image fusion. Generally, the procedure of wavelet-based image fusion includes the following steps: (1) decompose the

panchromatic image into a set of lower resolution wavelet coefficients; (2) replace the approximation coefficient with a multispectral band at the same resolution level; and (3) perform IDWT back to the original panchromatic resolution level to generate one band of the fused image. The replacement and IDWT are conducted three times, one for each multispectral band, to obtain the fused image. It has been reported that the color distortion of the fused image can be reduced to some extend with wavelet-based fusion approaches (Wald *et al.* 1997, Zhou *et al.* 1998, Ranchin and Wald 2000). However, the color often does not appear smoothly integrated into the spatial features (Zhang 2002).

Image Fusion with Wavelet-Enhance IHS Transform Method

Similar to the FFT-enhanced IHS transform method, the basic idea behind the wavelet-enhanced IHS transform method is to modify the input high-resolution panchromatic image so that it looks more like the intensity component of the input multispectral image. Instead of using a total replacement of the intensity component, this method uses a partial replacement based on a wavelet transform, where the high frequency part of the intensity component is replaced with the high-resolution wavelet coefficients from the panchromatic image. Again, the modified intensity component, together with the original hue and saturation components, are transformed back to the RGB color space, resulting in a fused image (Figure 3.4). The procedure for image fusion using the wavelet-enhanced IHS transform method is outlined in Table 3.3.

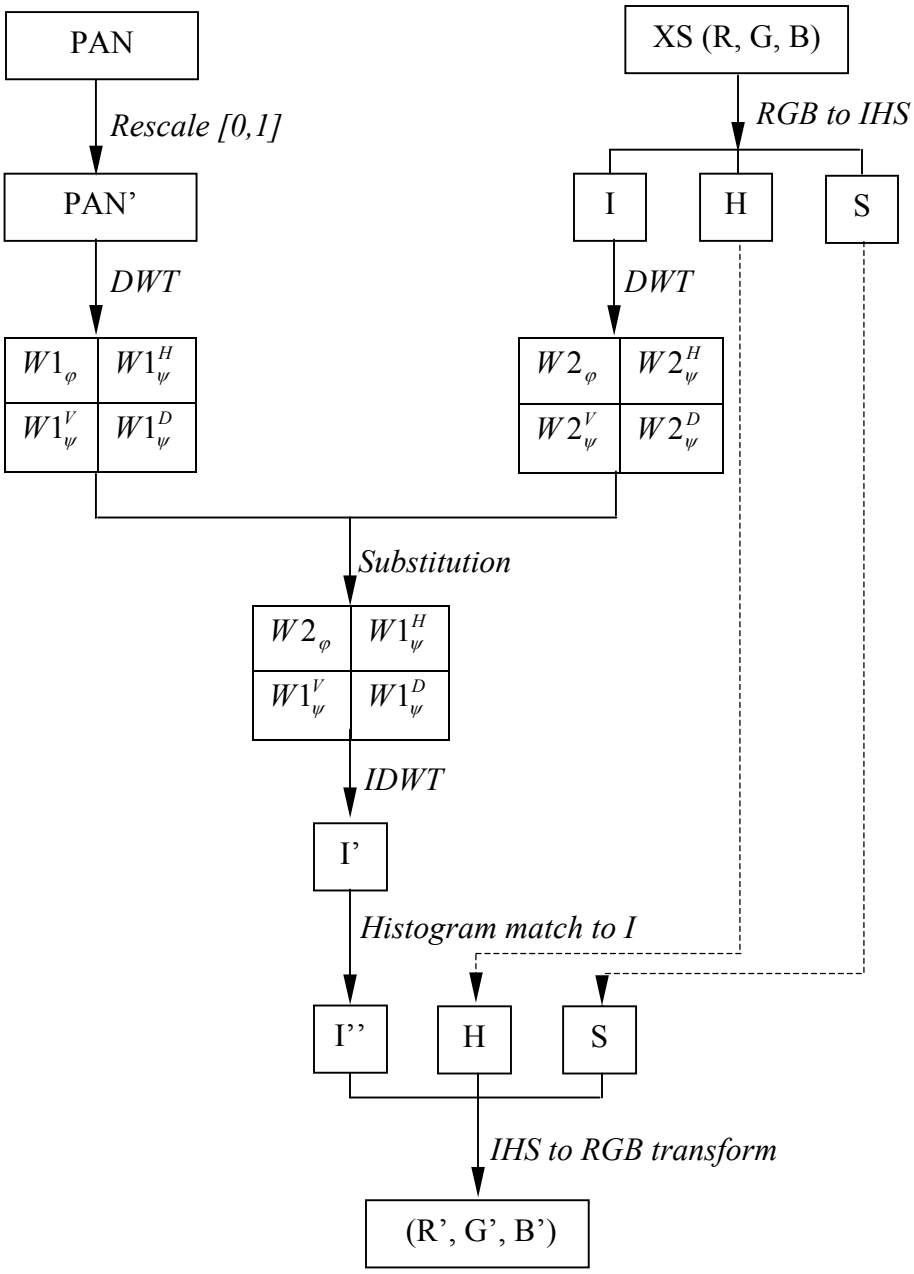

Figure 3.4: Schematic diagram for the wavelet-enhanced IHS transform method.

Table 3.3: The Procedure of Image Fusion Using the Wavelet-Enhanced IHS Transform Method.

1	Register all images to the panchromatic image and resample to the highest resolution (e.g., Ikonos 1-m, QuickBird 0.61-m) using cubic convolution.
2	Transform the resampled multispectral image from RGB to IHS color space to obtain the intensity (*I*), hue (*H*), and saturation (*S*) components.
3	Rescale the panchromatic image to [0,1] and decompose it to four components: approximation coefficients $W1_{\varphi}$, horizontal coefficients $W1_{\psi}^{H}$, vertical coefficients $W1_{\psi}^{V}$, and diagonal coefficients $W1_{\psi}^{D}$.
4	Decompose the intensity image to four components: approximation coefficients $W2_{\varphi}$, $W2_{\psi}^{H}$, $W2_{\psi}^{V}$, and $W2_{\psi}^{D}$.
5	Replace $W1_{\varphi}$ with $W2_{\varphi}$ and perform an inverse discrete wavelet transform (IDWT) on $W2_{\varphi}$, together with $W1_{\psi}^{H}$, $W1_{\psi}^{V}$, and $W1_{\psi}^{D}$, to create a new intensity image *I'*.
6	Match *I'* to the original *I* to obtain a new intensity component, *I''*.
7	Perform an IHS to RGB transform on *I''*, together with the original hue (*H*) and saturation (*S*) components, to create the fused image.

Experiments and Results

To assess the quality of the fused images, fusion results from different techniques should be evaluated visually, spectrally and spatially (Zhou *et al.* 1998). Change in spectral characteristics is an indication of the change in radiometric content of the image. Minimizing distortion of the spectral characteristics is important since this ensures that features spectrally separable in the original dataset are still separable in the fused dataset (Chavez *et al.* 1991). In this study, different comparisons are conducted to evaluate the enhanced IHS transform methods by comparing the fused images with the outputs obtained from the traditional IHS transform and PCA methods. First, the fused images are compared to the original images using visual means. Then histograms of the fused images are checked and compared to those of the original multispectral images. To quantify the spectral and spatial changes, inter-band correlations and the correlations between the panchromatic image and other bands of the multispectral image are analyzed for both the fused images and the original multispectral images. Finally the correlation

coefficient and band discrepancy between the fused image and corresponding original multispectral image are calculated to assess the spectral quality of the fused images. The coefficient between the intensity component of the fused image and that of the panchromatic image is used as a measure to assess the spatial quality. Test data consist of Ikonos and QuickBird images over the Camp Lejeune study area. The tested fusion methods include the FFT-enhanced IHS transform, the wavelet-enhanced IHS transform, the traditional IHS transform, and the PCA methods.

Fusion of Ikonos Images

Figure 3.5 shows the fusion results of the Ikonos images. A representative portion of the whole image showing a vegetated and bare ground area was selected for comparison of the fusion techniques. Figures 3.5*a* and 3.5*b* are the original Ikonos panchromatic image and multispectral image, respectively. The fused images from the FFT-enhanced and the wavelet-enhanced IHS transform methods are shown in Figures 3.5*c* and 3.5*d*, respectively. Figures 3.5*e* and 3.5*f* are the fused images from the traditional IHS transform and the PCA methods.

Visual comparison reveals that all four fused images inherited high spatial information from the panchromatic image. As for spectral quality, Figures 3.5*c* and 3.5*d* preserve the spectral characteristics and appearance of bare ground and vegetation in the original multispectral image. For example, the dark green area, labeled with letter *A*, has almost the same color and brightness in Figures 3.5*c* and 3.5*d* as that in the original multispectral image 3.5*b*. By contrast, in Figures 3.5*e* and 3.5*f* – the conventional IHS and PCA fused images – the bare ground areas (*A*) appear reddish brown and vegetation (*B*) a darker red. Wetland and damp soil are also easily distinguished. Thus, in this instance, the apparent color distortion associated with IHS and PCA images works to the advantage of the interpreter.

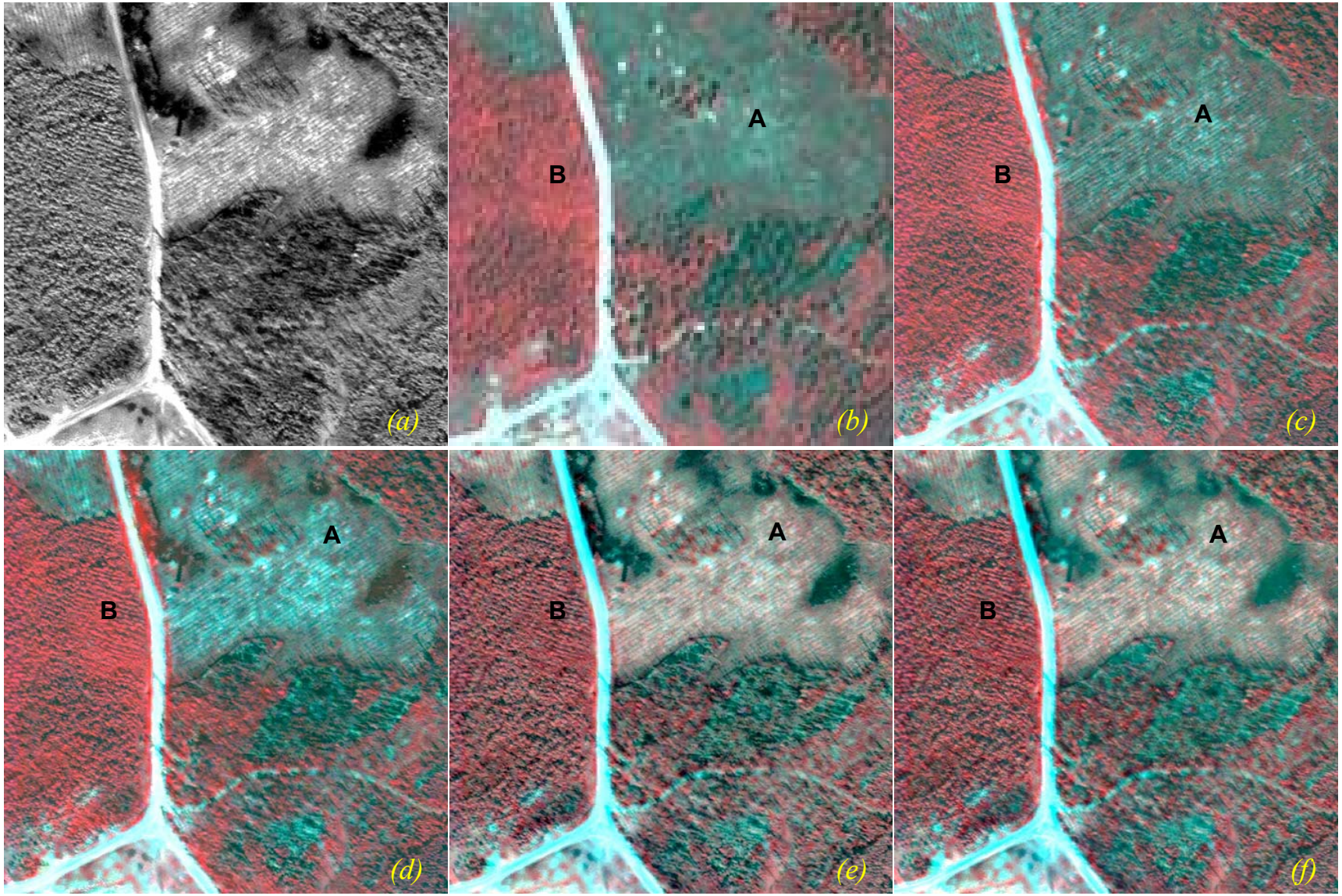

Figure 3.5: The Original and fused Ikonos images: (a) Ikonos panchromatic image (1 m); (b) Ikonos multispectral image (4 m); (c) fused image from the FFT-enhanced IHS transform method (1 m); (d) fused image from the wavelet-enhanced IHS transform method (1m); (e) fused image from the IHS method (1 m); (f) fused image from the PCA method (1 m).

In addition to multiresolution data, this particular example demonstrates the fusion of multitemporal image data. The acquisition date of the input Ikonos Pan image was 20 May 2000, while the multispectral image was acquired a year later on 27 August 2001. The input multispectral image, therefore, represents the most current condition of the landscape and may explain the difference in color between the IHS/PCA and FFT/wavelet enhanced methods. Specifically, in the conventional IHS and PCA methods, since the intensity component is totally replaced by the panchromatic image, the color information of the original multispectral image is modified by the panchromatic image. On the other hand, the color information is well preserved in the fused images from FFT and wavelet-enhanced IHS transform methods because only the high frequency part of the panchromatic image is fused to the multispectral image. In the cases when the panchromatic image represents the most up-to-date condition, one may adjust the filtering in the enhanced methods accordingly. From this point of view, the FFT and wavelet-enhanced IHS methods are more flexible than conventional IHS and PCA methods.

To compare with the original multispectral image, the fused images are resampled to a resolution of the original multispectral image. Ideally, when a fused image is resampled to its original resolution, the resulting image should be as close as possible to the original image (Ranchin and Wald 2000). Checking the histograms of the fused images after resampling and comparing them with those of the original multispectral image provides a quantitative test of this property. Histograms of the original multispectral image and the fused images are presented in Figure 3.6. It can be seen from the figure that the histograms of the fused image from the FFT-enhanced IHS transform and the wavelet-enhanced IHS transform methods retain the broad normal distribution and character, and are closer to those of the original image than those from the traditional IHS transform and the PCA methods.

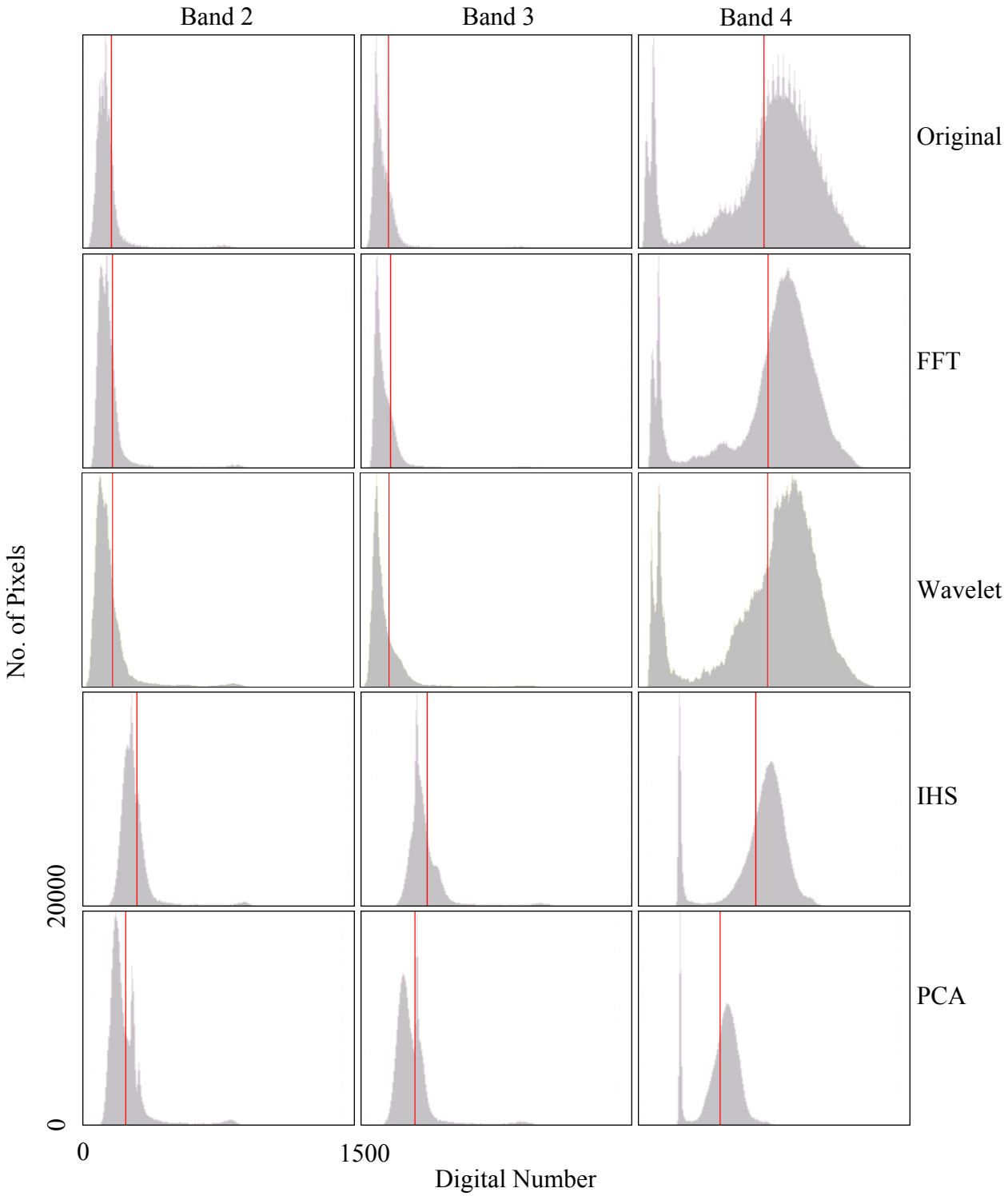

Figure 3.6: Histograms of the original multispectral and fused images from the FFT-enhanced IHS method, the wavelet-enhanced IHS method, the IHS transform method, and the PCA method. The first column is for band 2, the second column is for band 3, and the last column is band 4.

Inter-band correlation is another property that should be preserved in image fusion. Carper *et al.* (1990) used this property to quantify the spectral changes resulting from image fusion. Table 3.4 compares the inter-band correlation of the fused images to that of the original multispectral image. While the differences are slight, the fused images from the FFT-enhanced IHS transform and the wavelet-enhanced IHS transform methods have more similar inter-band correlation to that of the original multispectral image than the inter-band correlations from IHS transform and PCA methods. This also is true from the analysis of correlation between the panchromatic image and each band of the multispectral image, as shown in Table 3.5.

Table 3.4: Inter-Band Correlation for the Original Multispectral and Fused Ikonos Images.

	Band2 & Band3	Band2 & Band4	Band3 & Band4
Original image	0.98	0.17	0.26
FFT-enhanced IHS	0.98	0.17	0.27
Wavelet-enhance IHS	0.98	0.17	0.27
IHS	0.98	0.20	0.32
PCA	0.98	0.09	0.18

Table 3.5: Correlation between the Panchromatic Image and Other Bands for the Original Multispectral and Fused Ikonos Images.

	Pan & Band2	Pan & Band3	Pan & Band4
Original	0.57	0.65	0.62
FFT-enhanced IHS	0.60	0.67	0.66
Wavelet-enhance IHS	0.60	0.65	0.65
IHS	0.61	0.69	0.82
PCA	0.50	0.56	0.85

The correlation coefficients and band discrepancy between the original image bands and corresponding bands of the fused images also are used to assess the spectral quality of the fused image (Li *et al.* 2002). The band discrepancy D_k is computed as

$$D_k = \frac{1}{n}\sum_i \sum_j |V'_{kij} - V_{kij}| \qquad (3.10)$$

where V'_{kij} and V_{kij} are the pixel values of the fused image and corresponding original multispectral image, respectively; k is the kth band and i, j are the ith row and the jth column, respectively; and n is the total number of pixels in the images. A small discrepancy between the fused image and the corresponding original multispectral image is desired. The correlation coefficient and band discrepancy between each original band and corresponding band of the fused images are calculated and summarized in Tables 3.6 and 3.7. As seen from these tables, the FFT-enhanced IHS transform and the wavelet-enhanced IHS transform methods produce better results with higher correlation coefficients and less band discrepancy.

Table 3.6: Correlation Coefficients between the Original Multispectral and Fused Ikonos Images.

	Band 2	Band 3	Band 4
FFT-enhanced IHS	0.98	0.98	0.92
Wavelet-enhanced IHS	0.97	0.98	0.91
IHS	0.95	0.94	0.82
PCA	0.96	0.94	0.81

Table 3.7: Computed Band Discrepancy between the Original Multispectral and Fused Ikonos Images.

	Band 2	Band 3	Band 4
FFT-enhanced IHS	5.04	4.57	7.84
Wavelet-enhanced IHS	7.75	6.26	8.20
IHS	25.19	37.56	16.15
PCA	16.43	26.05	9.86

Note: Lower values indicate more similar images while higher values indicate more discrepancy.

Finally, the correlation coefficient between the intensity component of the fused image and the panchromatic image is used as a measure to assess the spatial quality of the fused image. Higher correlation between the intensity component of the fused image and that of the panchromatic image indicates that more spatial information from the panchromatic image is

incorporated during fusion. Table 3.8 presents the calculated correlation coefficient between the intensity component of the fused image and the panchromatic image. It shows that the fused images from the enhanced methods have higher spatial correlation, which indicates more information from the panchromatic image is incorporated in the fused images.

Table 3.8: Correlation Coefficient between the Intensity Component of the Fused Ikonos Image and the Ikonos Panchromatic Image.

FFT-enhanced IHS	0.987
Wavelet-enhanced IHS	0.976
IHS	0.890
PCA	0.791

Fusion of QuickBird Images

Figure 3.7 shows the fusion results of the QuickBird images of an urban-type setting within Camp Leujune. The original QuickBird panchromatic and multispectral images are shown in Figures 3.7*a* and 3.7*b*. Figures 3.7*c* and 3.7*d* are the fused images from the FFT-enhanced IHS transform and the wavelet-enhanced IHS transform methods, respectively. Again, Figures 3.7*e* and 3.7*f* are the fused images from the traditional IHS transform and the PCA methods. From the visual comparison, one can see that the colors in Figures 3.7*e* and 3.7*f* are somewhat different from those of the other fused images. Compared to the results from the Ikonos images, the color distortion in the fused IHS and PCA QuickBird images is more noticeable. This may indicate that as the spatial resolution increases, the color distortion becomes more serious in the fused image when traditional fusion techniques are applied.

Figure 3.8 compares the histograms of four fused images with that of the original multispectral image, and Tables 3.9 to 3.13 give the results from statistical comparisons. Once again it is evident that the FFT-enhanced IHS transform and the wavelet-enhanced IHS

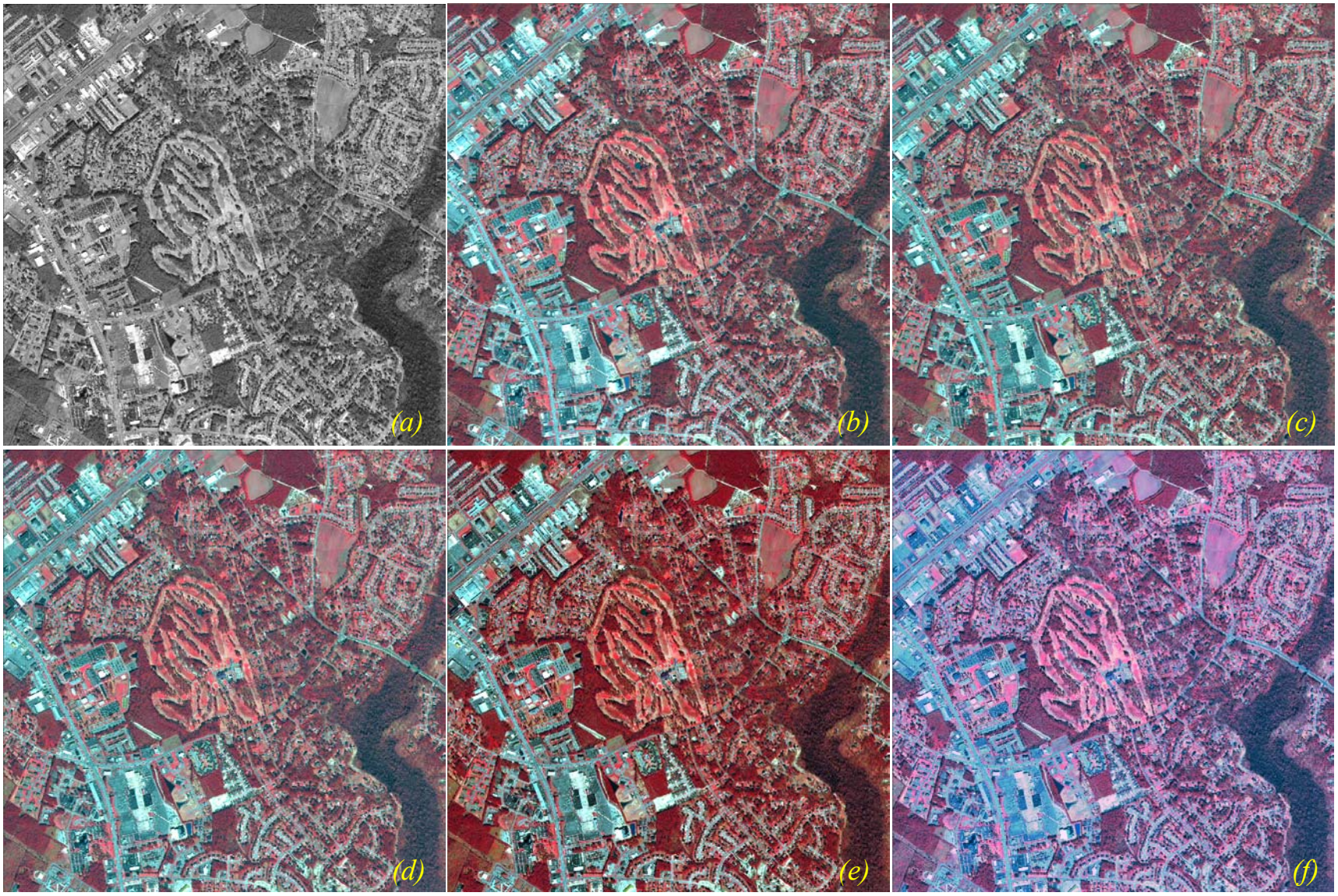

Figure 3.7: The original and fused QuickBird images: (a) QuickBird panchromatic image (0.61 m); (b) QuickBird multispectral image (2.44 m); (c) fused image from the FFT-enhanced IHS transform method (0.61 m); (d) fused image from the wavelet-enhanced IHS transform method (0.61 m); (e) fused image from the IHS method (0.61 m); (f) fused image from the PCA method (0.61 m).

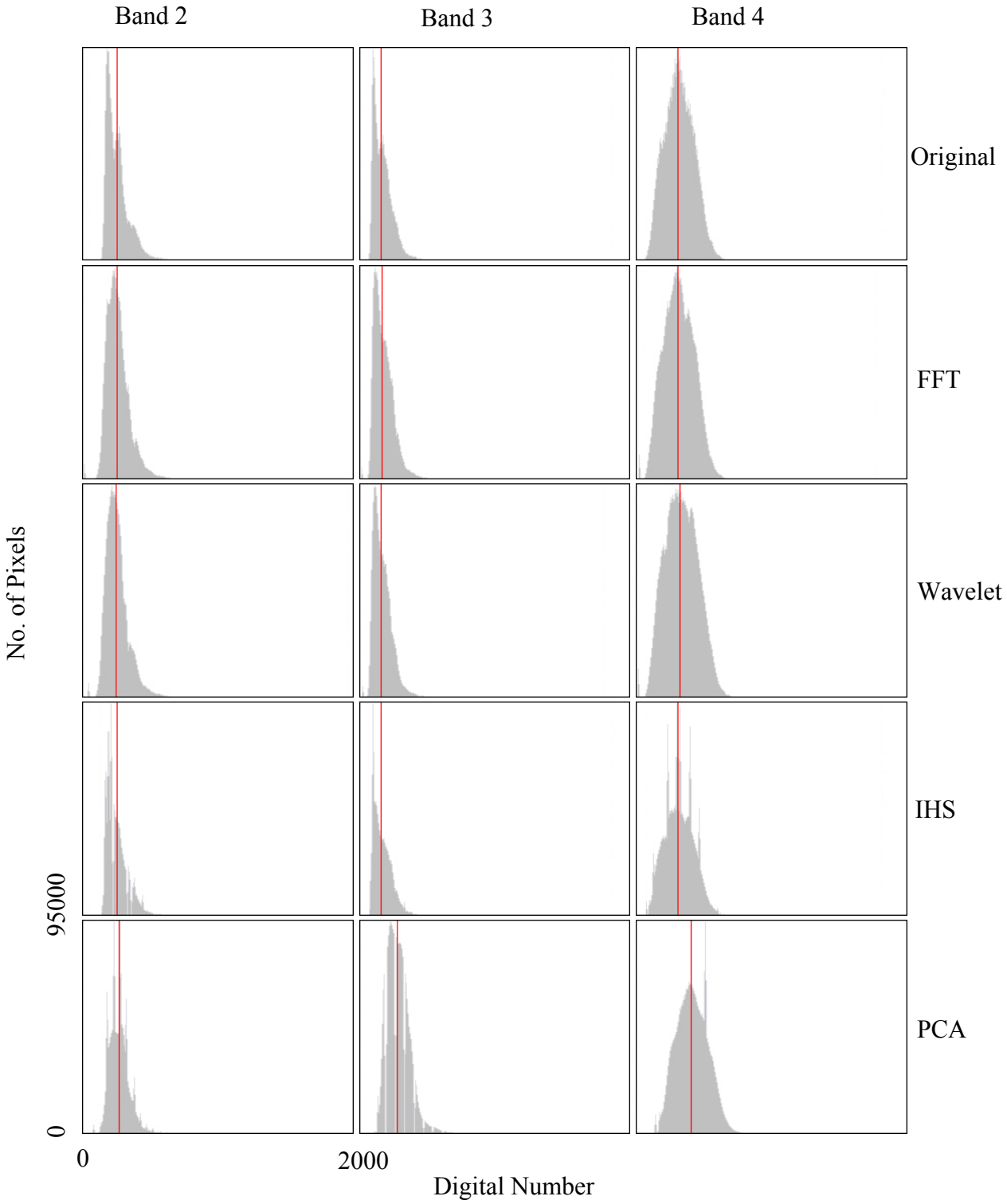

Figure 3.8: Histograms of the original QuickBird multispectral image and fused images from the FFT-enhanced IHS method, the wavelet-enhanced IHS method, the IHS transform method, and the PCA method. The first column is for band 2, the second column for band 3, and the last column band 4.

Table 3.9: Inter-Band Correlation for the Original and Fused QuickBird Images.

	Band2 & Band3	Band2 & Band4	Band3 & Band4
Original image	0.97	0.55	0.53
FFT-enhanced IHS	0.97	0.55	0.54
Wavelet-enhanced IHS	0.97	0.55	0.53
IHS	0.90	0.43	0.53
PCA	0.88	0.37	0.61

Table 3.10: Correlation between the Panchromatic Image and Other Bands for the Original and Fused QuickBird Images.

	Pan & Band2	Pan & Band3	Pan & Band4
Original	0.91	0.90	0.83
FFT-enhanced IHS	0.91	0.90	0.83
Wavelet-enhanced IHS	0.90	0.90	0.83
IHS	0.83	0.81	0.81
PCA	0.83	0.74	0.73

Table 3.11: Correlation Coefficients between the Original and Fused QuickBird Images.

	Band 2	Band 3	Band 4
FFT-enhanced IHS	0.94	0.88	0.89
Wavelet-enhanced IHS	0.92	0.88	0.83
IHS	0.73	0.69	0.73
PCA	0.62	0.61	0.79

Table 3.12: Computed Band Discrepancy between the Original and Fused QuickBird Images.

	Band 2	Band 3	Band 4
FFT-enhanced IHS	2.32	1.39	2.71
Wavelet-enhanced IHS	2.89	2.15	4.28
IHS	3.39	5.54	8.78
PCA	3.54	14.90	13.59

Table 3.13: Correlation Coefficient between the Intensity Component of the Fused QuickBird Image and the QuickBird Panchromatic Image.

FFT-enhanced IHS	0.98
Wavelet-enhanced IHS	0.97
IHS	0.87
PCA	0.83

transform methods may yield better results than the traditional IHS transform and PCA methods in terms of retaining the spectral and spatial values of the original image. It also shows that the fused image from the FFT-enhanced IHS transform method is slightly better than that from the wavelet-enhanced IHS transform method.

Conclusion

Two enhanced IHS transform methods have been presented in this paper to fuse the new generation high-resolution commercial satellite images. The FFT-enhanced IHS transform method combines a standard IHS transform with a FFT filtering of both the panchromatic image and the intensity component of the original multispectral image. The basic idea is to substitute the high frequency part of the intensity component only. Similarly, the wavelet-enhanced IHS transform method uses a partial replacement based on a wavelet-based technique, where high-resolution wavelet coefficients from the panchromatic image are fused to the multispectral image.

While inheriting the spatial integrity from the panchromatic image, these two enhanced IHS methods can preserve the spectral characteristics of the input multispectral image to a greater extent than the traditional IHS transform and PCA methods. This study also shows, when traditional IHS transform and the PCA methods are applied, the color distortion in the fused QuickBird images is more serious than that of the fused Ikonos images, especially for the vegetated areas. Between the two enhanced IHS transform methods, the FFT-enhanced IHS transform produces slightly better results than the wavelet-enhanced IHS transform method.

Further improvement of these two enhanced methods is to automate the best design of filters or wavelet transform functions to modify the intensity component of the original

multispectral image. Other approaches for quality assessment of the fused image, such as comparison of land-use maps obtained after spectral (and possibly textural) classification, also warrant future investigation.

Acknowledgements

Support for the Ikonos and QuickBird image data was provided by the Center for Remote Sensing and Mapping Science (CRMS), Department of Geography, the University of Georgia and the National Geospatial-Intelligence Agency (NGA) (formerly National Imagery and Mapping Agency (NIMA)) under the Cooperative Agreement NIMA 201-00-1-1006, Assessing the Ability of Commercial Sensors to Satisfy Littoral Warfare Data Requirements (NIMA 2002). The authors would like to express their appreciation to Dr. Roy Welch, Dr. Richard Brand, and Dr. Scott Loomer for their initiative and assistance throughout the project. We also gratefully acknowledge many individuals of the CRMS who worked on this project including Dr. Thomas Jordan, Dr. Jimmu Choi, Dr. Yanfen Le, Thomas Litts, and Virginia Vickery.

References

Carper, W.J., T.W. Lilesand, and R.W. Kieffer, 1990. The use of Intensity-Hue-Saturation transformation for merging SPOT panchromatic and multispectral image data, *Photogrammetric Engineering and Remote Sensing*, Vol. 56, No.4, pp. 459 – 467.

Chavez, P.S., S.C. Sides, and J.A. Anderson, 1991. Comparison of three different methods to merge multiresolution and multispectral data: TM & SPOT pan, *Photogrammetric Engineering and Remote Sensing*, Vol. 57, No. 3, pp. 295 – 303.

Cliche, G., F. Bonn, and P. Teillet, 1985. Integration of the SPOT Pan channel into its multispectral mode for image sharpness enhancement, *Photogrammetric Engineering and Remote Sensing*, Vol. 51, No. 3, pp. 311 – 316.

Ehlers, M., 1991. Multisensor image fusion techniques in remote sensing, *ISPRS Journal of Photogrammetry and Remote Sensing*, Vol. 46, pp. 19 – 30.

Gonzales, R. and R. Woods, 1992. *Digital Image Processing*, Addison-Wesley Publishing Company.

Jain, A.K, 1989. *Fundamentals of Digital Image Processing*, Englewood Cliffs, Prentice-Hall.

Li, S., J.T. Kwok, and Y. Wang, 2002. Using the discrete wavelet transform to merge Landsat TM and SPOT panchromatic images, *Information Fusion*, Vol. 3, No. 1, pp. 17 – 23.

Lillesand, T.M., R.W. Kiefer, and J.W. Chipman, 2004. *Remote Sensing and Image Interpretation*, 5th edition, John Wiley & Sons, 763 p.

Mallat, S.G., 1989. A theory for multiresolution signal decomposition: the wavelet representation, *IEEE Transactions on Pattern Analysis and Machine Intelligence*, Vol. 11, No. 7, pp. 674 – 693.

NIMA, 2002. *Assessing the Ability of Commercial Sensors to Satisfy Littoral Warfare Data Requirements, Agreement # NMA 201-00-1-1006* (January 18, 2002), Cooperative Agreement between NIMA and the UGA Foundation, National Imagery and Mapping Agency (NIMA), Washington, D.C., 5 p.

Onslow County, North Carolina, 2005. URL: http://www.onslowcountyschools.org/OCinfosheet.htm (last date accessed: 23 November 2005).

Price, J.C., 1987. Combining panchromatic and multispectral imagery from dual resolution satellite instruments, *Remote Sensing of Environment*, Vol. 21, No. 9, pp. 119 – 128.

Ranchin, T. and L. Wald, 2000. Fusion of high spatial and spectral resolution images: the ARSIS concept and its implementation, *Photogrammetric Engineering and Remote Sensing*, Vol. 66, No. 1, pp. 49 – 61.

Shettigara, V.K., 1992. A generalized component substitution technique for spatial enhancement of multispectral images using a higher resolution data set, *Photogrammetric Engineering and Remote Sensing*, Vol. 58, No. 5, pp. 561 – 567.

Smith, W.S., 1999. *The Scientist and Engineer's Guide to Digital Signal Processing*, California Technical Publishing, Second Edition, Chapter 9.

Tu, T.M., S.C. Su, H.C. Shyu, and P.S. Huang, 2001. A new look at IHS-like image fusion methods, *Information Fusion*, Vol. 2, No. 3, pp. 177 – 186.

Wald, L., T. Ranchin, and M. Magolini, 1997. Fusion of satellite images of different spatial resolutions: assessing the quality of resulting images, *Photogrammetric Engineering and Remote Sensing*, Vol. 63 No. 6, pp. 69 – 699.

Welch, R. and M. Ehlers, 1987. Merging multiresolution SPOT HRV and Landsat TM data, *Photogrammetric Engineering and Remote Sensing*, Vol. 53, No. 3, pp. 301 – 303.

Yesou, H., Y. Besnus, and J. Rolet, 1993. Extraction of spectral information from Landsat TM data and merger with SPOT panchromatic imagery – a contribution to the study of geological structures, *ISPRS Journal of Photogrammetry and Remote Sensing*, Vol. 48, No. 5, pp. 23 – 36.

Zhang, Y., 1999. A new merging method and its spectral and spatial effects, *International Journal of Remote Sensing*, Vol. 20, No. 10, pp. 2003 – 2014.

Zhang, Y., 2002. Automatic image fusion: A new sharpening technique for IKONOS multispectral images, *GIM International*, Vol. 16, No.5, pp. 54 – 57.

Zhou, J., D.L. Civco, and J.A. Silander, 1998. A wavelet transform method to merge Landsat TM and SPOT panchromatic data, *International Journal of Remote Sensing*, Vol. 19, No. 4, pp. 743 – 757.

CHAPTER 4

EFFECTS OF SPATIAL RESOLUTION RATIO IN IMAGE FUSION[1]

[1] Ling, Y, E.L. Usery, M. Ehlers, M. Madden, To be submitted to the *International Journal of Remote Sensing*.

Abstract

In image fusion, the spatial resolution ratio can be defined as the ratio between the pixel size of the high-resolution panchromatic image (1) and that of the low-resolution multispectral image (>1). This paper attempts to assess the effects of the spatial resolution ratio of the input images on the quality of the fused image. Experimental results indicate that a spatial resolution ratio of 1:10 or better is desired for optimal multisensor image fusion provided the panchromatic image is not resampled to a coarser resolution. Due to the synthetic pixels generated from resampling, the quality of the fused image decreases as the spatial resolution ratio decreases (e.g., from 1:10 to 1:30). However, even with a resolution ratio as small as 1:30, the quality of the fused image is still better than the original multispectral image alone. In cases where the spatial resolution ratio is too small (e.g., 1:30), to obtain better spectral integrity of the fused image, one may resample the high-resolution panchromatic image to a slightly lower resolution before fusing it with the multispectral image.

Introduction

Image fusion is a technique used to combine images of different resolutions, often a high-resolution panchromatic or radar image with a low-resolution multispectral image to improve interpretability. Ideally, the fused image inherits high-resolution spatial information from the panchromatic image and preserves original spectral characteristics of the multispectral image.

Methods have been developed in the past two decades for fusing panchromatic images of high spatial resolution with multispectral images of lower resolution (e.g., Cliche *et al.* 1985, Price 1987, Welch and Ehlers 1987, Chavez *et al.* 1991, Ehlers 1991, Shettigara 1992, Yesou *et*

al. 1993, Zhang 1999, Zhang 2002). Most of these methods emphasize the improvement in spatial resolution, while retaining the spectral integrity of the multispectral image. The objective of this study is to assess how the spatial resolution ratio of the input images affects the quality of the fused image.

Study Area and Image Data

The study area lies in Camp Lejeune, North Carolina (34° 35' N latitude, 77° 18' W longitude). Camp Lejeune is a large Marine Corps base, surrounding the estuary of the New River, on the Atlantic coast in southeastern North Carolina (Figure 4.1). The base consists of a

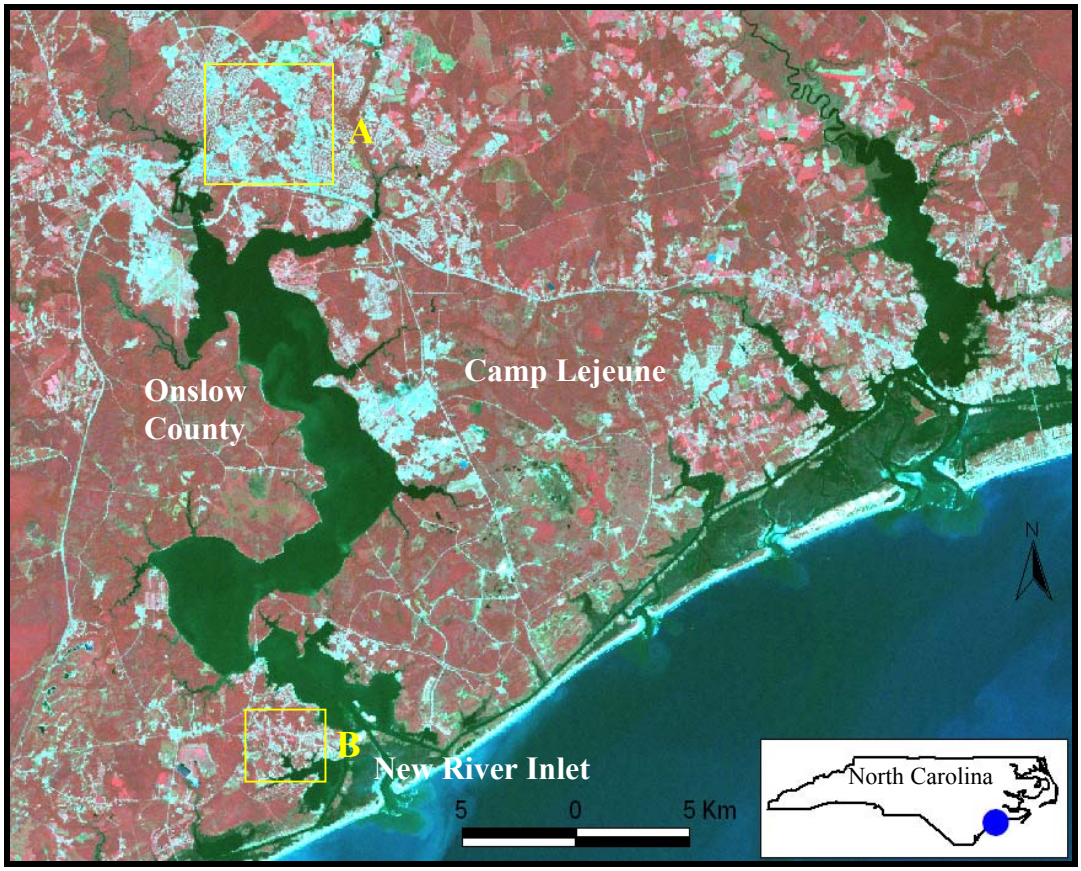

Figure 4.1: Camp Lejeune study area, North Carolina.

mix of natural areas, mainly planted pine and deciduous forests, and urban areas with medium-density residential areas, high-density military facilities and recreation areas such as golf courses.

Image data used in this study include an Ikonos dataset containing a panchromatic image and three multispectral image bands over the site marked *A* in Figure 4.1, and a SPOT panchromatic image and three bands of a Landsat ETM+ multispectral image over the site marked *B* in Figure 4.1 (Table 4.1). Resampled images derived from these original images also are used to create different resolution ratios during the fusion processes. All the images are spatially registered to the same Universal Transverse Mercator (UTM) coordinate system on the WGS 84 datum.

Table 4.1: Image Data Used in the Study.

Image data	Spectral bandwidth (μm)	Spatial resolution (m)	Acquisition date
SPOT Pan	0.51 – 0.73	10	5/20/1996
Landsat ETM+ XS (Bands 2, 3, 4)	Band 2: 0.53 – 0.61 Band 3: 0.63 – 0.69 Band 4: 0.78 – 0.90	30	9/23/1999
Ikonos Pan	0.45 – 0.90	1	2/5/2000
Ikonos XS (Bands 2, 3, 4)	Band 2: 0.51 – 0.60 Band 3: 0.63 – 0.70 Band 4: 0.76 – 0.85	4	8/27/2001

Methodology

Image Fusion Method

Among the variations of image fusion techniques, two of the most popular and effective ones are intensity-hue-saturation (IHS) transform and principal components analysis (PCA) methods (Zhang 1999, Tu *et al.* 2001). The IHS fusion converts a multispectral image in red-green-blue (RGB) color space into the IHS color space. Because the intensity component (I)

resembles a panchromatic image, it is replaced by a high-resolution panchromatic image in the fusion. A reverse IHS transform is then performed on the panchromatic image, together with the original hue (H) and saturation (S) components, to obtain the fused image.

For the PCA fusion method, the transformation determines a set of eigenvalues and eigenvectors, applies them in a linear combination with the original image bands and converts inter-correlated bands of a multispectral image into a new set of uncorrelated components. The first component, containing the most variance, is similar to a panchromatic image. It is, therefore, replaced by a high-resolution panchromatic image for the fusion. The fused image is obtained by performing a reverse PCA transform.

In this study, the IHS transform method is adopted for the fusion if the spatial resolution (i.e., pixel size) of the input images is poorer than 10 metres. For the cases with a spatial resolution better than 10 metres, the *fast Fourier transform* (*FFT*)*-enhanced IHS transform method* (Ling *et al.* 2006) is employed for the fusion. The FFT-enhanced IHS transform method combines the standard IHS transform method and FFT filtering, where only the high-frequency part of the intensity component is replaced with that of the panchromatic image.

Fusion Experiments

Three experiments involving five fusion cases with different resolution ratios were conducted (Table 4.2). These are discussed in the following paragraphs.

Experiment I: SPOT Pan – Landsat ETM+ XS fusion and Ikonos Pan – XS fusion

Fusions of a SPOT panchromatic (Pan) and a Landsat ETM+ multispectral (XS) image, as well as Ikonos Pan and multispectral images, are among the most popular fusions in remote sensing with many successful applications reported (Welch and Ehlers 1987, Yesou *et al.* 1993, Zhang 2002, Ling *et al.* 2006). The resolution ratios for these two fusion cases are 10:30 (or 1:3)

Table 4.2: Fusion Experiments Designed in the Study.

Experiment	Fusion case		Input images	Resolution ratio	Fusion method
I	1	SPOT Pan – Landsat ETM+ XS fusion	SPOT Pan (10 m) Landsat ETM+ XS (30 m)	10:30 (1:3)	IHS transform
	2	Ikonos Pan – XS fusion	Ikonos Pan (1 m) Ikonos XS (4 m)	1:4	FFT-enhanced IHS transform
II	3	Ikonos Pan – resampled 10-m, 20-m, and 30-m Ikonos XS images	Ikonos Pan (1 m) Resampled Ikonos XS (10 m, 20 m, and 30 m)	1:10, 1:20, and 1:30	FFT-enhanced IHS transform
III	5	Ikonos 1-m Pan image and Pan images resampled to 5 m, 10 m – Landsat ETM+ XS image	Ikonos Pan (1 m) Resampled Ikonos Pan (5 m, 10 m), Landsat ETM+ XS (30m)	1:30, 5:30 (1:6), and 10:30 (1:3)	FFT-enhanced IHS transform and IHS transform

and 1:4, respectively. In the SPOT Pan – Landsat ETM+ XS fusion, the spatial resolution of SPOT Pan is 10 metres and of Landsat ETM+ XS is 30 metres. The Landsat ETM+ XS image was resampled to 10-m resolution using a cubic convolution algorithm before it was fused with the SPOT Pan image. A standard IHS transform method was applied to this fusion and the fused image has a spatial resolution of 10 metres. In the Ikonos Pan – XS fusion, the spatial resolutions of Ikonos Pan and XS image are 1 and 4 metres, respectively. The multispectral image was resampled to 1-m resolution using cubic convolution before it was fused with the Ikonos Pan image. The *FFT-enhanced IHS method* was applied to this fusion and the fused image has a spatial resolution of 1 metre.

Experiment II: Ikonos Pan with resampled 10-m, 20-m, and 30-m Ikonos XS images

The objective of Experiment II is to examine how the quality of the fused image changes as the resolution ratio decreases. The Ikonos XS image was first resampled to 10-m, 20-m, and 30-m resolution. These resampled images were used as simulated multispectral data to fuse with the Ikonos 1-m Pan image. Therefore, the resolution ratios are 1:10, 1:20, and 1:30, respectively. The simulated multispectral images were then resampled to 1-m resolution using cubic convolution before fusing with the Ikonos Pan image. The *FFT-enhanced IHS method* was applied to these fusion cases and the fused images have a spatial resolution of 1 metre.

Experiment III: Ikonos 1-m Pan image and Pan image resampled to 5 m and 10 m with Landsat ETM+ XS image

The objective of Experiment III is to examine how the fusion result changes as we trade spatial and spectral resolution. In this experiment, the 1-m resolution Ikonos Pan image was first resampled to 5-m and 10-m resolution images. Then the Ikonos Pan and the two resampled images were fused with a 30-m Landsat ETM+ XS image, respectively. Therefore, the

resolution ratios for these fusion cases are 1:30, 5:30 (1:6) and 10:30 (1:3), respectively. The *FFT-enhanced IHS* method was applied to the first two fusion cases and the standard IHS transform method to the last one. The fused images have spatial resolutions of 1, 5, and 10 metres, respectively.

Results and Discussion

In this section, visual and statistical comparisons are conducted to evaluate the fused images of various resolution ratios. In visual comparison, the spectral characteristics and spatial structures of the fused image are compared to those of the original multispectral image. Histograms of the fused images also are examined and compared to those of the original images. In statistical comparison, the correlation coefficient between the fused image and the corresponding original multispectral image is calculated to assess the spectral quality of the fused images.

Fusion Results for Experiment I

Figures 4.2 and 4.3 show the results of SPOT Pan – Landsat ETM+ XS and Ikonos Pan – XS fusions. Visual comparisons between the original multispectral images and the fused images reveal that the fused images inherited high spatial information from the panchromatic image. Both fused images also have similar color information to the corresponding original multispectral images. For example, in Figure 4.2, the spatial quality of linear features such as roads and river channels is much clearer in the fused image than in the original multispectral image, while the spectral information has been retained. In Figure 4.3, the urban structures are greatly enhanced in the fused image. The edges of the buildings have been sharpened. Similar

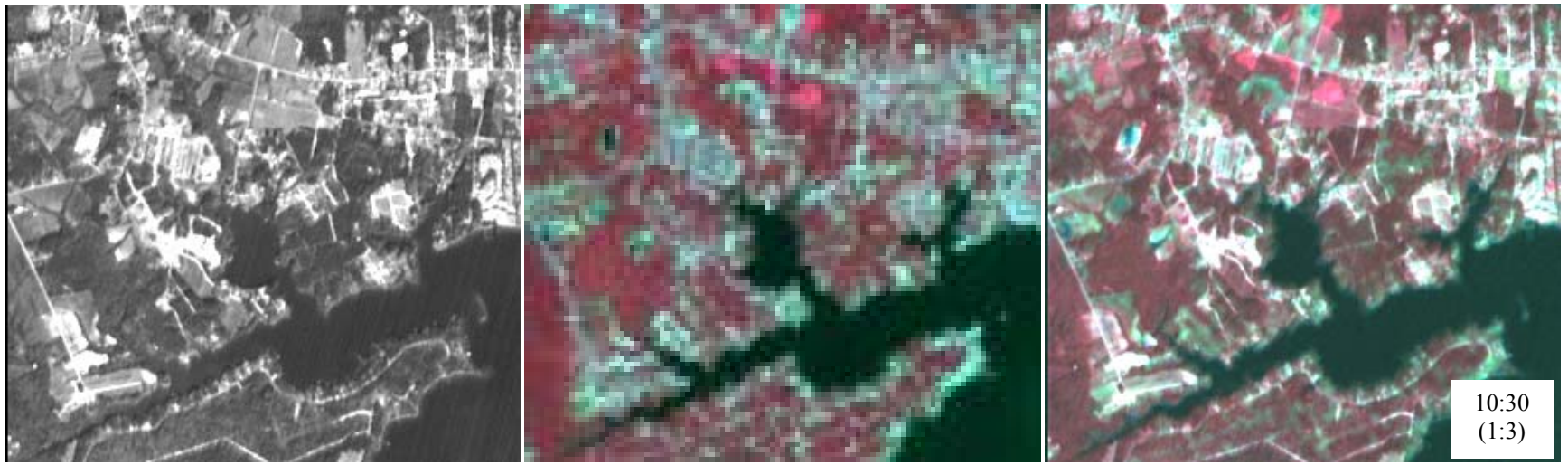

a (10 m) b (30 m) c (10 m)

Figure 4.2: The original and fused images for *SPOT Pan – Landsat ETM+ XS* fusion: (a) SPOT Panchromatic image; (b) a color composite of original Landsat-ETM+ bands 2, 3, and 4; (c) fused image using the IHS transform method.

Original multispectral image (4 m) Fused image (1 m)

Figure 4.3: A representative portion of the original multispectral and fused images in the *Ikonos Pan – XS* fusion.

sharpening occurs with roads with the center stripe and road edges becoming apparent in the fused image. Also, the fused image has more detailed texture information for the vegetated areas than the original multispectral image.

Histograms of the original multispectral images and the fused images are presented in Figure 4.4 and show both fused images have similar histograms to that of the corresponding original multispectral images. From the point of statistical analysis, Table 4.3 illustrates the correlation coefficients between fused images and original multispectral images. The high correlation coefficients (all greater than 0.83) indicate that the spectral properties of the original multispectral images are successfully preserved in the fused images. This means that satisfactory fusion results can be achieved when we use a 10:30 (1:3) resolution ratio for SPOT Pan – Landsat ETM+ XS fusion and 1:4 for Ikonos Pan – XS fusion.

Table 4.3: Correlation Coefficient between the Original Multispectral and Fused Images in Experiment I.

	Band 2	Band 3	Band 4
SPOT Pan – Landsat ETM+ XS fusion	0.85	0.85	0.83
Ikonos Pan – XS fusion	0.95	0.94	0.91

Fusion Results for Experiment II

Figures 4.5 and 4.6 show the results of Experiment II. The 10-m, 20-m, and 30-m multispectral images resampled from the original Ikonos multispectral image are given in Figure 4.5. A representative portion of the fused images in Figure 4.6 indicates that, as the resolution ratio decreases (i.e., from 1:10 to 1:30), the quality of the fused image decreases and more artifacts appear in the fused image. These fusion results also show that, even when the resolution ratio is as small as 1:30, the fused image is still better than the original multispectral image alone (See Figures 4.5*c* and 4.6*c*). Artifacts in the fused image were introduced as the spatial resolution

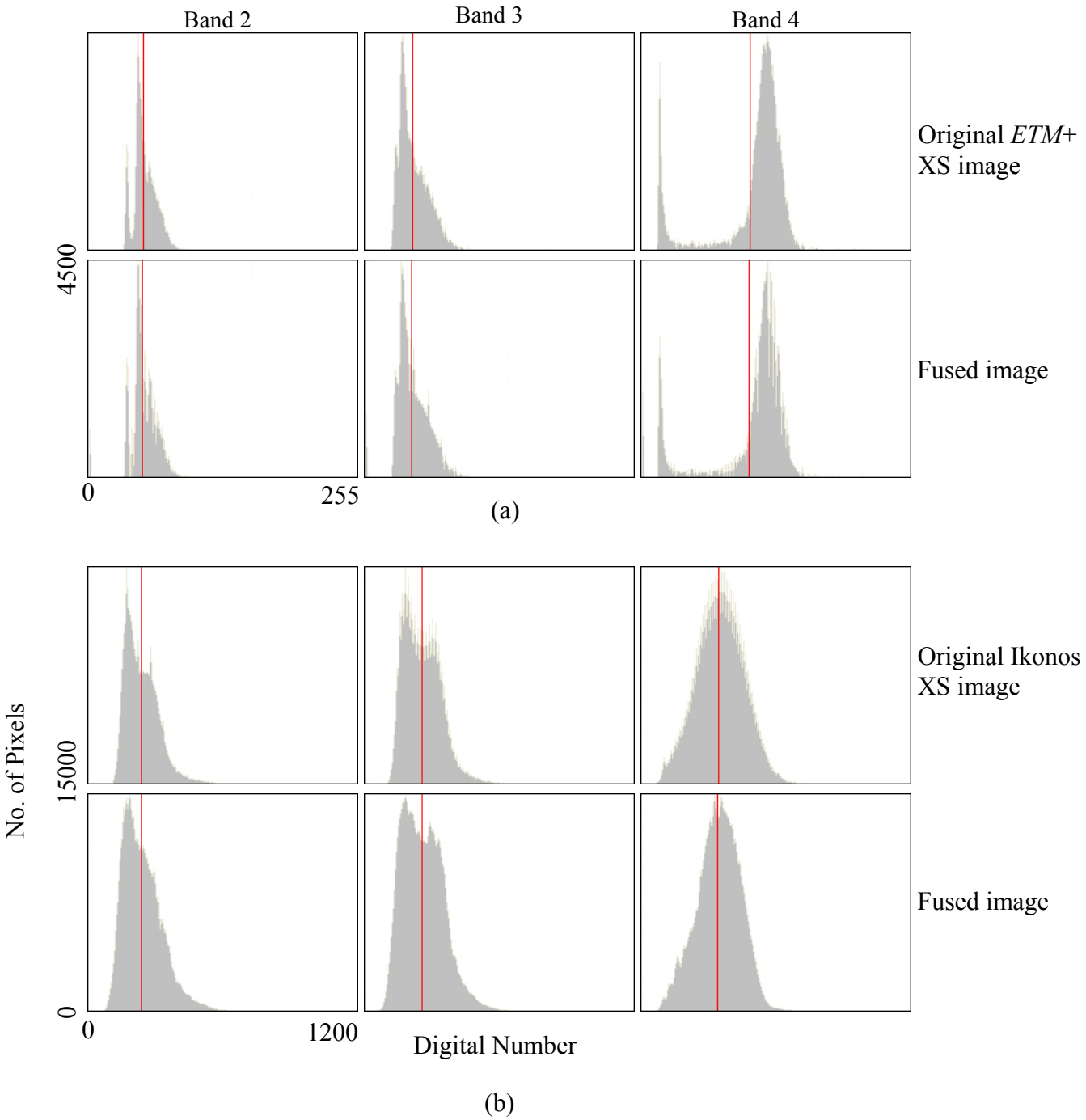

Figure 4.4: Histograms of the original multispectral and fused images in experiment I: (a) histograms for the original Landsat ETM+ XS image (the first row) and the fused image (the second row); (b) histograms for the original Ikonos multispectral image (the third row) and the fused image (the fourth row).

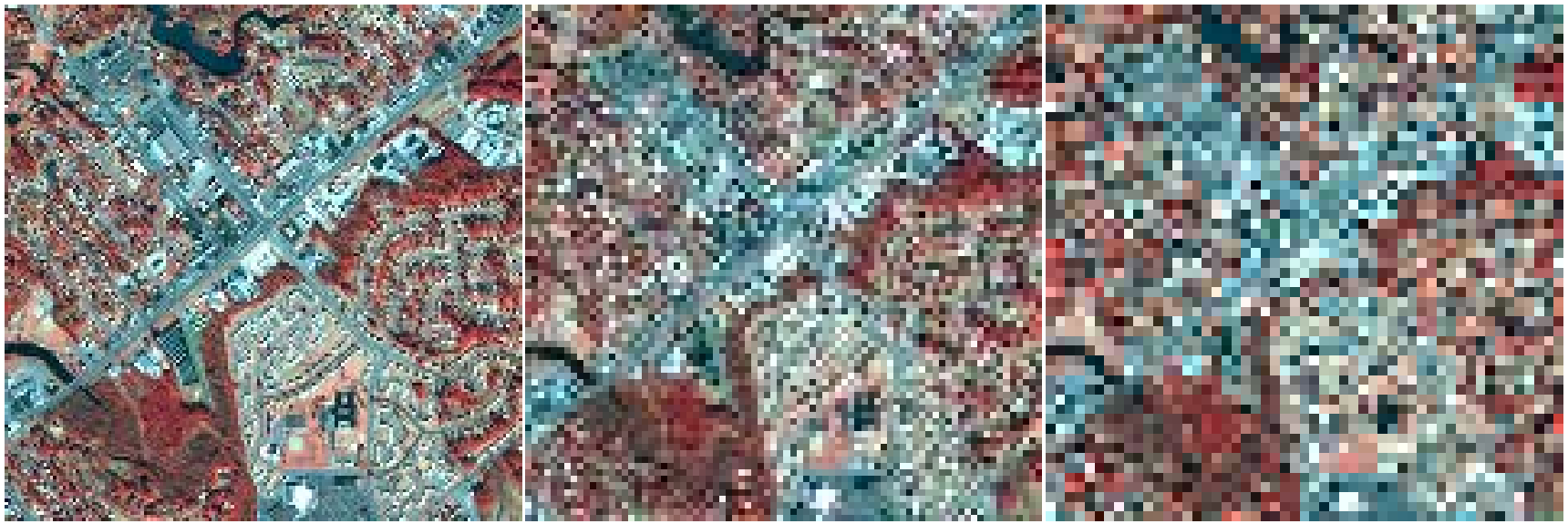

a (10 m) b (20 m) c (30 m)

Figure 4.5: Multispectral images resampled from Ikonos 4-m multispectral image: (a) resampled 10-m resolution XS image; (b) resampled 20-m resolution XS image; (c) resampled 30-m resolution XS image.

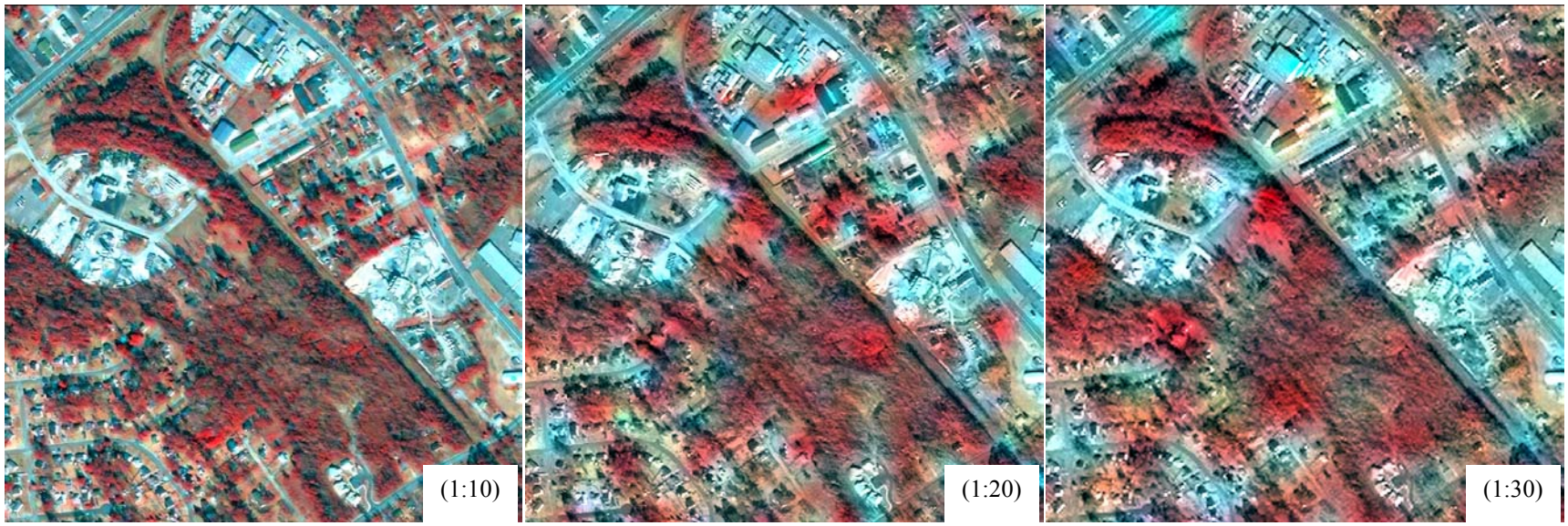

a (1 m) b (1 m) c (1 m)

Figure 4.6: A representative portion of results from fusing Ikonos 1-m Pan with resampled 10-m, 20-m, and 30-m Ikonos XS images: (a) result from fusing with resampled 10-m resolution XS image; (b) result from fusing with resampled 20-m resolution XS image; (c) result from fusing with resampled 30-m resolution XS image.

of the multispectral image decreased. This is because more synthetic pixels were generated during resampling before the multispectral image was fused with the high-resolution panchromatic image. These synthetic pixels do not represent any natural or man-made objects and often cause distortion of the shape of real features. Table 4.4 illustrates the correlation coefficients between the original and fused images. Correlation coefficients decrease as the resolution ratio decreases due to the presence of synthetic pixels in the fused image.

Table 4.4: Correlation Coefficient between the Original Multispectral and Fused Images in Experiment II.

	Band 2	Band 3	Band 4
Ikonos Pan with resampled 10-m XS image	0.92	0.92	0.90
Ikonos Pan with resampled 20-m XS image	0.89	0.82	0.82
Ikonos Pan with resampled 30-m XS image	0.78	0.78	0.73

Fusion Results for Experiment III

The results for fusing Ikonos 1-m, resampled 5-m and 10-m Pan images with Landsat ETM+ XS image are depicted in Figures 4.7a, 4.7b, and 4.7c, respectively. From visual comparison, one cannot identify much difference between 4.7a and 4.7b. As the Ikonos Pan resampled to 10-m resolution, many artifacts, such as the white spots in urban areas, are introduced into the fused image. From the statistical analysis, Table 4.5 shows that, although the spatial resolution of the Ikonos Pan decreases from 1 m to 5 m, the correlation coefficient between the original multispectral image and the fused image does not decrease. The coefficients indicate that Figure 4.7b even preserves slightly better spectral characteristics of the original Landsat ETM+ multispectral image than Figure 4.7a. The quality of Figure 4.7c, however, is worse than the other two because of the introduced artifacts during the resampling. The compromise of spatial resolution for spectral quality of the fused image shown in this experiment

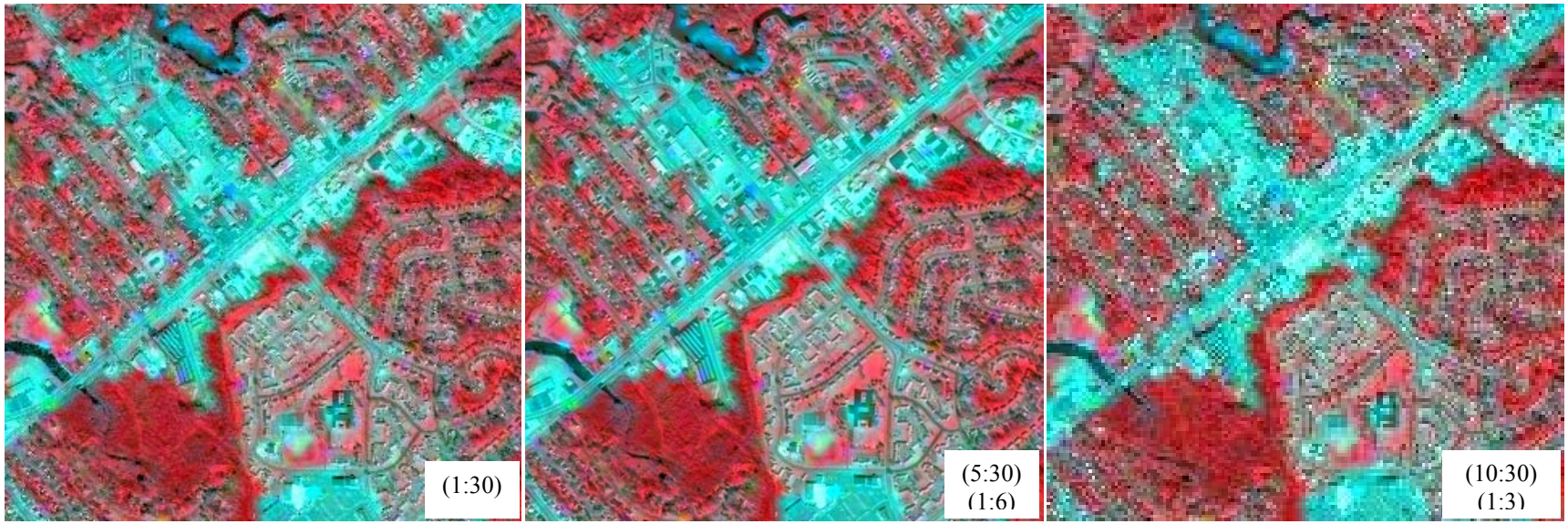

a (1 m) b (5 m) c (10 m)

Figure 4.7: Results from fusing Ikonos 1-m, resampled 5-m, 10-m Pan images with Landsat ETM+ XS image: (a) result from fusing Ikonos 1-m Pan with Landsat ETM+ XS image; (b) result from fusing resampled 5-m Ikonos Pan with Landsat ETM+ XS image; (c) result from fusing resampled 10-m Ikonos Pan with Landsat ETM+ XS image.

may be helpful to some studies in which spectral quality is critical and extreme high spatial resolution is not necessary. Therefore, in some cases, if the resolution ratio is small (i.e., 1:30 in this case), one may resample the panchromatic image to a slightly lower resolution before fusing it with the multispectral image in order to obtain better spectral properties of the fused image.

Table 4.5: Correlation Coefficient between the Original Multispectral and Fused Images in Experiment III.

	Band 2	Band 3	Band 4
1m Ikonos Pan with 30-m Landsat ETM+ XS	0.76	0.88	0.74
5m Ikonos Pan with 30-m Landsat ETM+ XS	0.78	0.89	0.78
10m Ikonos Pan with 30-m Landsat ETM+ XS	0.67	0.73	0.65

Conclusion

Visual comparisons and statistical analyses of fused images show that a resolution ratio of 1:10 or better is needed for successful multisensor image fusion provided the panchromatic image not resampled to a coarser resolution. Generally, the quality of the fused image decreases as the resolution ratio decreases (e.g., from 1:10 to 1:30). However, even when the resolution ratio is as small as 1:30, the fused image is still better than the original multispectral image alone. On the other hand, due to the synthetic pixels generated in resampling, more artifacts are introduced to the fused image as the resolution ratio decreases. When the resolution ratio is small (for example 1:30), one might need to compromise the spatial resolution of the fused image to obtain better spectral quality by resampling the high-resolution panchromatic image to a slightly lower resolution before fusing it with the multispectral image. In the case of resampling the panchromatic image to 10 m, even though the effective resolution ratio was 1:3, the image quality was not superior.

Acknowledgements

Support for the Ikonos and QuickBird image data was provided by the Center for Remote Sensing and Mapping Science (CRMS), Department of Geography, the University of Georgia and the National Geospatial-Intelligence Agency (NGA) (formerly National Imagery and Mapping Agency (NIMA)) under the Cooperative Agreement NIMA 201-00-1-1006, Assessing the Ability of Commercial Sensors to Satisfy Littoral Warfare Data Requirements (NIMA 2002). The authors would like to express their appreciation to Dr. Roy Welch, Dr. Richard Brand, and Dr. Scott Loomer for their initiative and assistance throughout the project. We also gratefully acknowledge many individuals of the CRMS who worked on this project including Dr. Thomas Jordan, Dr. Jimmu Choi, Dr. Yanfen Le, Thomas Litts, and Virginia Vickery.

References

Chavez, P.S., S.C. Sides, and J.A. Anderson, 1991. Comparison of three different methods to merge multiresolution and multispectral data: TM & SPOT pan, *Photogrammetric Engineering and Remote Sensing*, Vol.57, No. 3, pp. 295 – 303.

Cliche, G., F. Bonn, and P. Teillet, 1985. Integration of the SPOT Pan channel into its multispectral mode for image sharpness enhancement, *Photogrammetric Engineering and Remote Sensing*, Vol. 51, No. 3, pp. 311 – 316.

Ehlers, M., 1991, Multisensor image fusion techniques in remote sensing, *ISPRS Journal of Photogrammetry and Remote Sensing*, 46, pp. 19 – 30.

Ling, Y., M. Ehlers, E.L. Usery, and M. Madden, 2006. Enhanced IHS transform methods for fusing commercial high-resolution satellite images, to be submitted to *ISPRS Journal of Photogrammetry and Remote Sensing*.

NIMA, 2002. *Assessing the Ability of Commercial Sensors to Satisfy Littoral Warfare Data Requirements, Agreement # NMA 201-00-1-1006* (January 18, 2002), Cooperative Agreement between NIMA and the UGA Foundation, National Imagery and Mapping Agency (NIMA), Washington, D.C., 5p.

Price, J. C., 1987. Combining panchromatic and multispectral imagery from dual resolution satellite instruments, *Remote Sensing of Environment*, Vol. 21, No. 9, pp. 119 – 128.

Shettigara, V. K., 1992. A generalized component substitution technique for spatial enhancement of multispectral images using a higher resolution data set, *Photogrammetric Engineering and Remote Sensing*, Vol.58, No. 5, pp. 561 – 567.

Tu, T.M., S.C. Su, H.C. Shyu, and P.S. Huang, 2001. A new look at IHS-like image fusion methods, *Information Fusion*, Vol. 2, No. 3, pp. 177 – 186.

Welch, R., and M. Ehlers, 1987. Merging multiresolution SPOT HRV and Landsat TM data, *Photogrammetric Engineering and Remote Sensing*, Vol. 53, No. 3, pp. 301 – 303.

Yesou, H., Y. Besnus, and J. Rolet, 1993. Extraction of spectral information from Landsat TM data and merger with SPOT panchromatic imagery – a contribution to the study of geological structures, *ISPRS Journal of Photogrammetry and Remote Sensing*, Vol. 48, No. 5, pp. 23 – 36.

Zhang, Y., 1999. A new merging method and its spectral and spatial effects, *International Journal of Remote Sensing*, Vol. 20, No. 10, pp. 2003 – 2014.

Zhang, Y., 2002. Automatic image fusion: A new sharpening technique for IKONOS multispectral images, *GIM International*, Vol.16, No. 5, pp. 54 – 57.

CHAPTER 5

SUMMARY AND CONCLUSION

A number of new generation commercial high-resolution satellite systems equipped with advanced imaging sensors have been launched in recent years. The successful commercial launches of the Ikonos, QuickBird, and OrbView-3 satellites in 1999, 2001, and 2003, respectively, offer the geospatial information communities important new sources of timely and accurate spatial information that can augment data provided by the public-sector remote sensing systems. The commercial satellites currently acquire images in two modes: a panchromatic mode with a high spatial resolution and a multispectral mode with a slightly coarser resolution. To extend the potential of such images, image fusion techniques that can effectively combine the merits of high spatial resolution of the panchromatic image and high spectral resolution of the multispectral image are desired. In this study, two advanced image fusion techniques: the FFT-enhanced IHS transform method and the wavelet-enhanced IHS transform method, are developed for use with commercial high-resolution satellite images. Both methods are tested using Ikonos and QuickBird image data. The improvement in spatial resolution and the retention of spectral fidelity are assessed for both methods via visual and statistical comparisons. This research also assesses how the spatial resolution ratio of input images affects the quality of the fused image.

Two classic image fusion techniques, the IHS transform and the PCA methods, have demonstrated most promising results for fusing radar or SPOT panchromatic images with Landsat TM and other multispectral images. However, they may not satisfy conditions for

successful fusion of the new generation satellite images such Ikonos and QuickBird data with spatial resolutions of approximately 0.5 to 4 meters. A notable color distortion often occurs in the fused image. It has been discussed that the major reason for the color distortion of fusing the new generation high-resolution commercial satellite images is the change of the panchromatic spectral range. Different from the SPOT panchromatic channel, the wavelength range of the Ikonos and QuickBird panchromatic channels was extended from visible to near infrared range. This change makes the gray value relationship of an Ikonos or QuickBird panchromatic image significantly different from that of a SPOT panchromatic image.

The FFT-enhanced IHS transform method combines the standard IHS transform with a FFT filtering of both the panchromatic image and the intensity component of the original multispectral image. The basic idea behind this method is to modify the input high-resolution panchromatic image so it looks more like the intensity component of the input multispectral image. Instead of using a total replacement of the intensity component as in the traditional IHS transform method, the FFT-enhanced IHS transform method uses a partial replacement based on a FFT filtering. The wavelet-enhanced IHS transform method combines the traditional IHS transform and a discrete wavelet transform for image fusion. It uses a partial replacement based on a wavelet-based technique, where only high frequency information of the intensity component is replaced by the high-resolution wavelet coefficients from the panchromatic image. Ikonos and QuickBird image data are used to assess these two enhanced IHS methods. Visual and statistical comparisons of the fused images demonstrate that these two enhanced IHS methods produce better results than the traditional IHS transform and the PCA methods in preserving the spectral characteristics of the input multispectral image while inheriting the spatial integrity of the panchromatic data. This study also shows, when traditional IHS transform and the PCA methods

are applied, the color distortion appeared in the fused QuickBird images is more serious than that of the fused Ikonos images, especially for vegetated areas. Between the two enhanced IHS transform methods, the FFT-enhanced IHS transform produces slightly better results than the wavelet-enhanced IHS transform method.

To assess how the spatial resolution ratio of the input images affects the fused image, experiments with varying resolution ratios of the input images were conducted and the quality of the fused images was evaluated. It has been shown that a resolution ratio no less than 1:10 is needed for optimal multisensor image fusion provided the panchromatic image is not resampled to a coarser resolution. In general, the quality of the fused image decreases as the resolution ratio decreases (for example, from 1:10 to 1:30). It has also been demonstrated that, even with a resolution ratio as small as 1:30, the fused image is still better than the original multispectral alone. On the other hand, due to the synthetic pixels generated in resampling, more artifacts are introduced to the fused image as the resolution ratio decreases. In cases when the resolution ratio is too small, for example, 1:30, one might need to compromise the spatial resolution of the fused image to obtain better spectral quality by resampling the panchromatic image to a slightly lower resolution (e.g., from 1 m to 5 m) before fusing it with the multispectral image.

With newer generation high-resolution remotely sensed data from commercial sensors available to public and private communities, it is anticipated that image fusion will be increasingly used and play an important role in remote sensing and geospatial applications. This research provided two advance techniques for fusing commercial high-resolution image data. Further improvement of these two methods is to automate the best design of filters or wavelet transform functions to modify the intensity component of the original multispectral image. Other issues related to this research also warrants future investigation. These includes quality

assessment using spectral classification, the cost of image fusion, and the suitability of these two enhanced IHS methods for fusing hyperspectral, radar, and LIght Detection And Ranging (LIDAR) data.